



Contents lists available at ScienceDirect

Tectonophysics

journal homepage: www.elsevier.com/locate/tecto

Eurasia Basin and Gakkel Ridge, Arctic Ocean: Crustal asymmetry, ultra-slow spreading and continental rifting revealed by new seismic data

A.M. Nikishin^a, C. Gaina^{b,*}, E.I. Petrov^c, N.A. Malyshev^d, S.I. Freiman^a

^a Geological Faculty, Moscow State University, Moscow, Russia

^b Centre for Earth Evolution and Dynamics, CEED, Department of Geosciences, University of Oslo, Norway

^c Rosnedra, MNR, Moscow, Russia

^d Rosneft, Moscow, Russia

ARTICLE INFO

Keywords:

Arctic Ocean
Eurasia Basin
Gakkel Ridge
Oceanic crustal asymmetry
Gakkel Ridge Deep
Khatanga-Lomonosov Fault

ABSTRACT

High Arctic new seismic data, collected by Russian Federation from 2011 to 2014, and additional geological and geophysical information, are used to interpret the basement and sedimentary structure of central and eastern Eurasia Basin, the Gakkel Ridge, and their transition into the Laptev Sea. We find that significant changes in basement topography occur in Nansen Basin at C20 (43.43 Ma) and in the Amundsen basins at C21 (45.7 Ma), and in both basins at C13 (33 Ma). A long seismic profile, that documents for the first time the structure of conjugate flanks and their margins in the central-eastern Eurasia Basin, confirms that oceanic accretion was asymmetric, with 10% less crust developed in the Amundsen Basin since continental break-up. In the eastern Amundsen Basin, we observe mid-ocean ridge uplift since C13 (33 Ma). We identify four distinct sedimentary packages in the Eurasia Basin: Early to Mid Eocene (c. 56 to 45.7 Ma), Mid Eocene to Early Oligocene (45.7 to 33.2 Ma), Early Oligocene to Early Miocene (33.2 to 19.7) and Early Miocene to Present (19.7 to 0 Ma); they are linked to the oceanic lithosphere age determined from magnetic data.

The deepest part of the Gakkel Ridge (5215 m), situated close to the easternmost part of this mid ocean ridge, is imaged for the first time by seismic data that reveals volcanic constructions within the older axial ridges and on the flanks. Gakkel Ridge's asymmetric flanks with shallow, regularly-spaced, and rugged structure, typical to ultra-slow spreading ridges, imply periodicity of tectonic phases. The Khatanga-Lomonosov Fault between Lomonosov Ridge and the Laptev Sea region, is identified on few seismic profiles; kinematic models predict that it may have been active only for a maximum of 10 myr after continental break-up.

1. Introduction

Two main basins, the Eurasia and the Amerasia basins, are located in the deep-water part of the Arctic Ocean, and are separated by the Lomonosov Ridge continental sliver. The present day plate boundary, the Gakkel Ridge (GR), previously known as Nansen cordillera (e.g. Beal et al., 1966), runs through the Eurasia Basin (Fig. 1), and is considered the slowest mid-ocean ridge on Earth (6–13 mm/yr, e.g. Jokat et al., 2003; Savostin et al., 1984; Dick et al., 2003). This plate boundary is connected on one side to the North Atlantic mid-ocean ridge through a narrow passage between Svalbard and Greenland, and on the other side to the Laptev Sea continental rifting (Fig. 1). Early studies of the Eurasia Basin at the beginning of the last century (with bathymetric measurements performed during the famous 1895 Nansen expedition) were followed by numerous oceanographic measurements by Russian scientists, who discovered the Lomonosov and the Gakkel

ridges by c. 1950, and by more intensive data acquisition campaigns in the subsequent decades. Sea ice covering this region for > 10 months per year, impedes data collection by ships; and the proximity to the North Pole (and north magnetic pole) complicates magnetic measurements. However, geological and geophysical data acquired by ships, airplanes, submarines and satellites before 2011 (Fig. 2) satisfactorily document the western part of the Eurasian Basin, including the western segment of the ultra-slow Gakkel Ridge, and can be used to identify the first order structure of the entire Eurasia Basin and surroundings.

The Eurasia Basin is floored by c. 57–0 Ma old oceanic crust (Karasik et al., 1983; Brozena et al., 2003; Glebovsky et al., 2006; Alvey et al., 2008); as inferred from the linear magnetic anomalies (Savostin and Karasik, 1981; Karasik et al., 1983; Savostin et al., 1984; Gaina et al., 2002; Brozena et al., 2003; Glebovsky et al., 2006; Gaina et al., 2014, 2015). The Gakkel Ridge started its magmatic activity in Late Paleocene-Early Eocene with an intermediate spreading rate (e.g.

* Corresponding author.

E-mail address: carmen.gaina@geo.uio.no (C. Gaina).

<http://dx.doi.org/10.1016/j.tecto.2017.09.006>

Received 2 June 2017; Received in revised form 4 September 2017; Accepted 9 September 2017
0040-1951/© 2017 Elsevier B.V. All rights reserved.

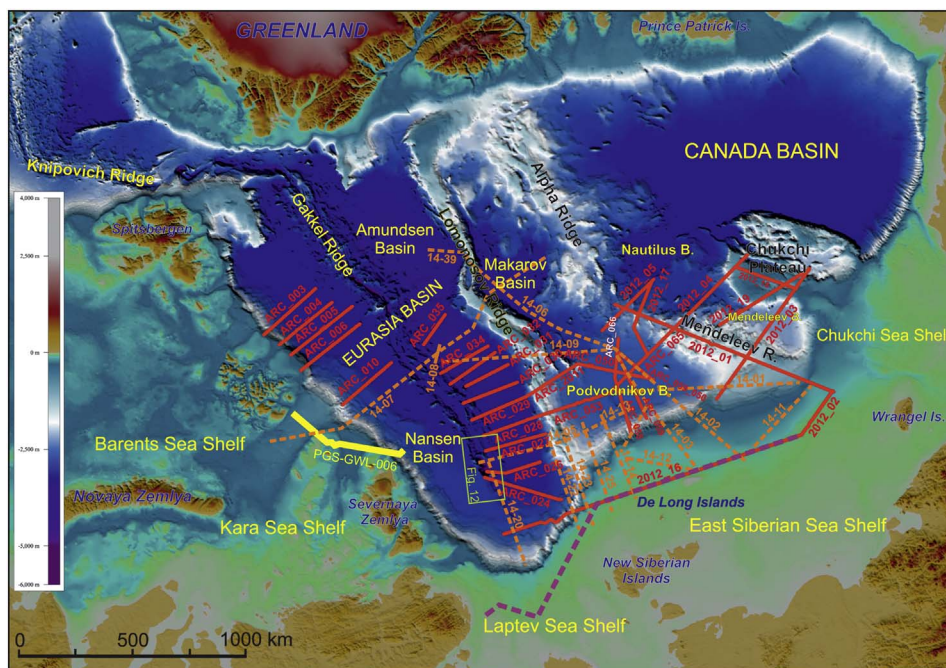


Fig. 1. Location and names of the new Russian Arctic seismic profiles used for the tectono-stratigraphic interpretation. Background map: Arctic topography and bathymetry (Jakobsson et al., 2012). Red lines are Russian Federal projects Arktika-2011 and Arktika-2012 seismic profiles, orange lines – Arktika-2014 seismic profiles, yellow line – “Geology Without Limits” selected profiles, purple lines – ION selected seismic profiles. (For interpretation of the references to colour in this figure legend, the reader is referred to the web version of this article.)

Brozena et al., 2003; Glebovsky et al., 2006).

The Nansen Basin and its continental margin (Fig. 1) has so far been the best-studied area of the Eurasia Basin due to denser than elsewhere geophysical data coverage. These studies have described: the Arctic plate boundary according to seismicity, bathymetry and potential field data (e.g. Engen et al., 2002), the segment of northern Barents Sea continental margin (e.g. Minakov et al., 2012), and the sedimentary cover of the western Eurasia Basin continental margin (e.g. Jokat and Micksch, 2004; Engen et al., 2009). In comparison, the Amundsen Basin (Fig. 1) was poorly studied (Jokat and Micksch, 2004; More and Pitman, 2011), and its continental margin, the Lomonosov Ridge, has only recently been described in some details (Chernykh and Krylov, 2011; Rekant and Gusev, 2012; Døssing et al., 2014). Until recently, the eastern part of the Eurasian Basin close to the Russian shelves of the Barents, Kara and Laptev seas (Fig. 1), had an extremely poor geophysical and geological data coverage (for a review see Drachev et al., 2010; Pease et al., 2014).

More recent data and interpretations of the Gakkel Ridge structure, mostly its western part, are presented in several studies (Schmidt-Aursch and Jokat, 2016; Morozov et al., 2016; Michael et al., 2003; Jokat et al., 2003; Urlaub et al., 2009; Jokat and Micksch, 2004; Cochran et al., 2003; Schlindwein et al., 2005, 2015; Jokat and Schmidt-Aursch, 2007; Cochran, 2008; Engen et al., 2009). Current knowledge indicates that the present day mid-ocean ridge has a very thin crust, c. 2–6 km thick (Urlaub et al., 2009; Schmidt-Aursch and Jokat, 2016), and is segmented in non-volcanic and sparsely-volcanic segments, with deep earthquakes in the amagmatic sections (at c. 35 km depth; Schlindwein and Schmid, 2016).

The past decade saw a substantial increase in the scientific and economic interest for the High Arctic. Concerted national and international expeditions collected large amounts of data from poorly surveyed areas, including the eastern part of the Eurasian Basin, and the surrounding continental margins and shelves. In 2011, 2012 and 2014, a total of 20,560 km of 2D seismic profiles was collected, using two icebreakers and a 600 m long streamer, by several multi-national research teams with major support from the Ministry of Natural Resources and Environment of the Russian Federation (see a subset of this data in Fig. 1). In 2012, Petroleum Geo-Services (PGS), together with scientific consortium Geology Without Limits, also launched a long-term international scientific survey of the Barents and Kara Seas

(for a review see Nikishin et al., 2013). The new data coverage surpasses any other systematic seismic investigation in the eastern (and probably in the entire) High Arctic.

For the first time, a large number of seismic data enables now to study the structure of the slowest part of the Gakkel Ridge, together with its oceanic flanks, and its continuation into the rifted Laptev Sea and neighboring areas. While part of the new Russian data was published by us (Nikishin et al., 2014, 2017; Gaina et al., 2015), or by our colleagues (Petrov et al., 2016; Rekant et al., 2015), this paper presents for the first time the detailed structure of the eastern Gakkel Ridge, Eurasia Basin and its continental margins as revealed by the new Russian seismic data, and a compilation of other existing data, in a plate tectonic context.

2. Regional tectonic framework

For setting the scene of the Eurasia Basin tectonic history, we will first review shortly the geology of continental crust to the south, east and north of this basin. The Eurasia Basin is bordered to the south by Barents and Kara sea shelves (Figs. 1, 2, 3) of Paleozoic and Neoproterozoic crust (e.g., Drachev et al., 2010; Pease et al., 2014; Nikishin et al., 2014). The Lomonosov Ridge tectonic sliver, detached from the northern Barents and Kara sea shelves in the Eocene, has presumably continental crust of the same age as these shelves (for a review see Poselov et al., 2012; Pease et al., 2014; Nikishin et al., 2014), and was modified by the orthogonally trending Silurian-Devonian Caledonian and Late Paleozoic Taimyr orogenies (Fig. 3).

The narrow plate boundary between the Eurasia and North American plates, the mid-ocean Gakkel Ridge, continues eastward within the stretched Laptev Sea continental domain. This continental rift system is a complex region of about 900 km width which started prior to the breakup between Lomonosov Ridge and the Barents/Kara sea shelves (Drachev et al., 1998, 2010; Sekretov, 2002; Franke et al., 2000, 2001; Zavarzina and Shkarubo, 2012; Nikishin et al., 2014, 2017; Khoroshilova et al., 2014; Mazur et al., 2015). The Laptev Sea continental basement is an amalgamation of terranes whose boundaries and ages are still disputed (Drachev et al., 2010; Drachev, 2016; Nikishin et al., 2014). The Ust’Lena Rift is probably underlain by the Verkhoyansk Mesozoic pre-Aptian fold belt (Drachev, 2016; Nikishin et al., 2017), but the connection between the Verkhoyansk and South Taimyr orogens is poorly documented. The South Anyui suture (e.g.

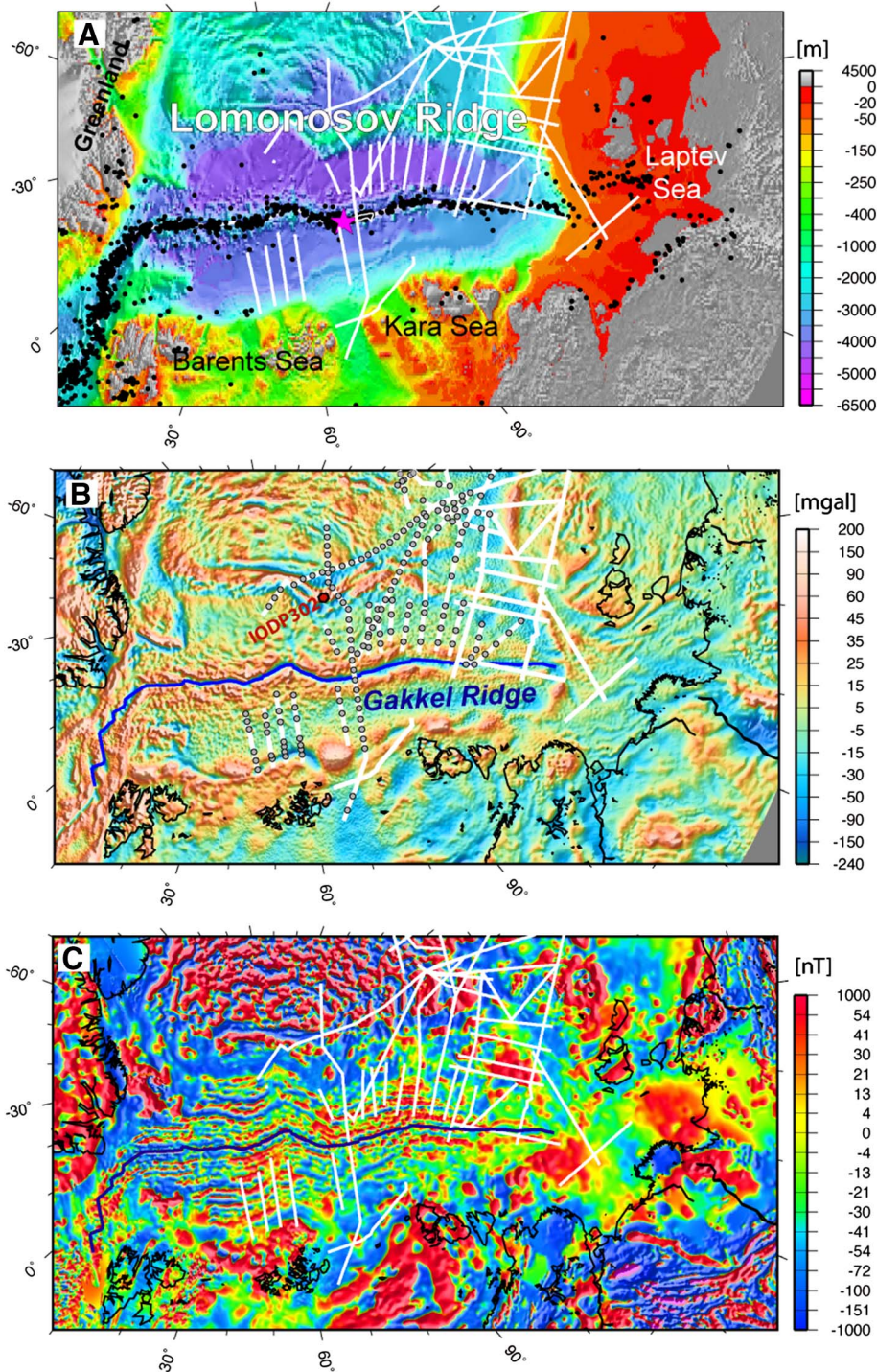


Fig. 2. Gridded geophysical data used in this study and location of Russian seismic profiles discussed in the text (in white): A. bathymetry (GEBCO2014/IBCAOV3); B. free air gravity anomalies (DTU13, Andersen et al., 2014); C. magnetic anomaly grid (CAMP-GM, Gaina et al., 2011). Gakkel Ridge location is from Engen et al. (2002). In panel A, black dots are earthquake locations from the ISC (www.isc.ac.uk/iscbulletin) and EMSC (www.emsc-csem.org) earthquake catalogues from 1960 to 2016. The latest large earthquake (magnitude 4.7) erupted on 22.10.2016 on the Gakkel Ridge is shown by the magenta star. Russian sonobuoy locations are shown as open circles (panel B). (For interpretation of the references to colour in this figure legend, the reader is referred to the web version of this article.)

Sokolov et al., 2002), formed between the East Siberian Shelf and Northeast Asia as the South Anyui Ocean was subducting, continues into the Laptev Sea, but its exact location is disputed (Kuzmichev, 2009; Drachev, 2016). On our tectonic map (Fig. 3), we draw the continuation of the South Anyui suture under the Bel'kov and Anisim rifts, following trends shown on the gravity and magnetic anomaly maps (Gaina et al., 2011), and based on interpretation of regional seismic lines. The New Siberian Islands terrane, with a Neoproterozoic basement overlain by a platform cover of Ordovician to Cenozoic age (Kos'ko et al., 2013; Nikishin et al., 2014; Ershova et al., 2016; Donukalova, 2016), is located north and east of the South Anyui suture. Fold deformations in these islands took place before the Aptian (Kos'ko et al., 2013). The De

Long Rise terrane is situated north of the New Siberian Islands terrane. A Neoproterozoic continental crust with a Cambrian-Ordovician sedimentary cover (Kos'ko et al., 2013; Donukalova, 2016), has been described in the southern part of this terrane, whereas north of it, lies a deformed Cambrian-Ordovician volcanic arc (Kos'ko et al., 2013; Ershova et al., 2016). The Zhokhov buried thrust belt of pre-Aptian age is imaged by seismic profiles between the New Siberian Islands and the De Long terranes (Drachev et al., 2010; Nikishin et al., 2014, 2017). Aptian deposits overlie the Zhokhov thrust belt and adjacent terranes above an angular unconformity. The Mesozoic deformation of this region may have ended before the Aptian time, and therefore we infer that the Laptev Sea rifting started not earlier than Aptian, but could

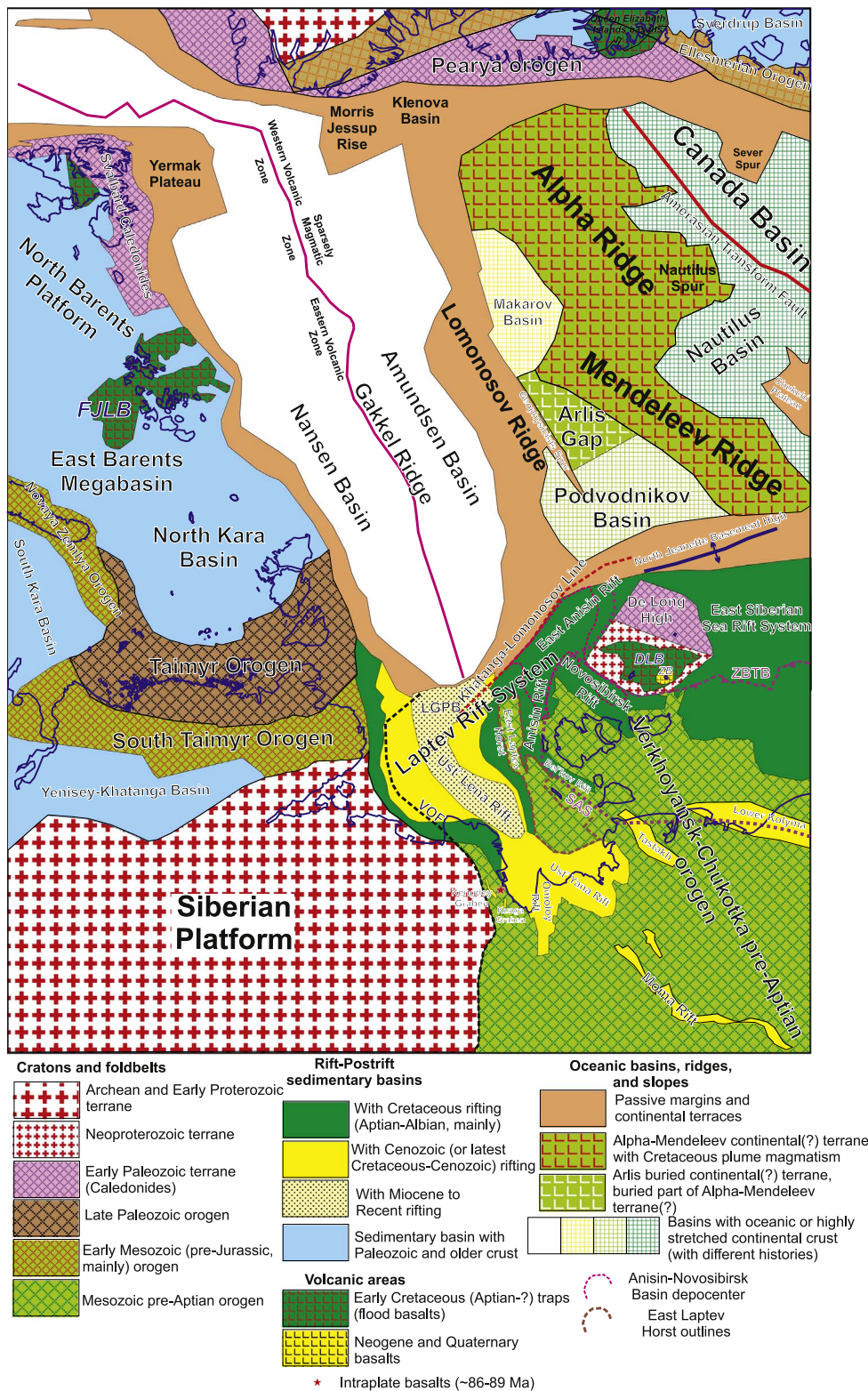


Fig. 3. High Arctic tectonic map revised after Nikishin et al. (2014, 2017). Abbreviations: DLB – De Long Basalts (128–112 Ma), LGPB – Laptev-Gakkel pull-apart basin (c. Oligocene to Recent), SAS – South Anyui Suture (c. 130–120 Ma), VOF – Verkhoyansk Orogen Front, ZB – Zhokhov Basalts (1–3.6 Ma), ZBTB – Zhokhov buried thrust belt.

have been as late as Turonian. According to Nikishin et al. (2017), the three main phases of Laptev Sea rifting are: (1) Aptian to Albian, (2) Paleocene (or at the end of Late Cretaceous-Paleocene), and (3) from Eocene to Quaternary (Fig. 3). It should be noted that there are no drilled wells in the Laptev Sea and the sediment stratigraphy can only be inferred from dated geological formation from the exposed islands and extrapolated from dated horizons in the Eurasia Basin (discussed in Section 4).

3. Data and methods

3.1. Seismic data

This study presents selected 2D seismic profiles collected in 2011, 2012 and 2014 in the High Arctic by two icebreakers. 214 sonobuoys have been deployed along seismic profiles (see Fig. 2 for their location). Details of seismic data acquisition are given in Table 1. Depth

Table 1
Seismic data acquisition technical details.

Seismic profiles	Streamer	Seismic source
ARC1407, ARC1408, ARC1409, ARC1406, ARC1439a, ARC1439	600 m length 48 channels, sampling rate 2 ms, recording length 12 s	8 airguns (total volume – 1300 dmq), shot interval 50 m
ARC1401, ARC1411, ARC1402, ARC1403, ARC1412, ARC1413, ARC1414, ARC1425, ARC1405, ARC1420	4500 m long 380 channels, sampling rate 2 ms, recording length 12 s	8 airguns (total volume - 1300 dmq), shot interval 50 m
ARC1216, ARC1202, ARC1201, ARC1205, ARC1217, ARC1204, ARC 1218	600 m long 48 channels, sampling rate 2 ms, recording length 15 s	8 airguns (total volume - 2050 dmq), shot interval 50 m
ARC1203, ARC1219	4500 m long 360 channels, sampling rate 2 ms, recording length 15 s	8 airguns (total volume - 2050 dmq), shot interval 50 m
ARC11 lines	600 m long 48 channels, sampling rate 2 ms, recording length 15 s	16 airguns (total volume - 2050 dmq), shot interval 50 m

Sonobuoy (Hydrophone - MP-24L3 from GeoSpace) data has been collected with a sampling rate of 4 ms, and a recording length of 8–12 s. The seismic source was a Bolt 8500APG, with 1300 dmq, at 50 m shot interval.

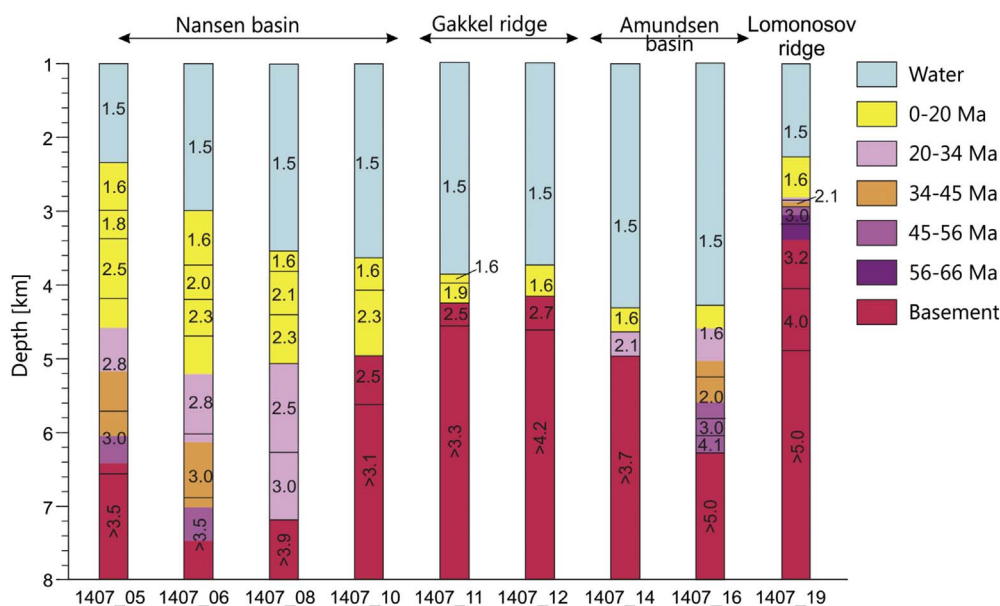


Fig. 4. Seismic velocity-depth model for the Nansen and Amundsen basins based on sonobuoy data recorded along profile ARC14-07 (see profile and sonobuoy location in Figs. 2 and 6).

conversion was performed with the software FOCUS and ECHOS (Paradigm Geotechnology) using information from seismic lines after time processing, regularization procedures and calculated velocity models with refined RMS velocities. For profiles with a long streamer (> 4500 m), velocity models were calculated from the reflected wave (CDP) velocity analysis. For profiles with a short streamer, velocity models were obtained from the sonobuoy refraction waves seismogram velocity analysis. A detailed analysis of all sonobuoy data will be published separately, but we document the velocity profiles used in depth conversion for the longest profile across the entire Eurasia Basin and its flanks (ARC14-07) in Fig. 4.

3.2. Potential field data

To assist with the interpretation of seismic data along selected profiles, we have used recently published bathymetry (GEBCO2014/IBCAOV3, www.gebco.net), and potential field data (magnetic data from the GAMPGM-M, 2 km resolution gridded data, Gaina et al., 2011; and free air gravity DTU13, 1 min resolution global grid, Andersen et al., 2014) as illustrated in Fig. 2. The Eurasia Basin magnetic gridded data is mainly based on the combined Russian (VNIIO)-American (NRL) gridded data published by Kovacs et al. (1999) and used by Glebovsky

et al. (2006) to interpret the kinematics of the Eurasian Basin. The original magnetic data distribution is published by Glebovsky et al. (2006), and we refer the reader to its Fig. 1.

The age of oceanic lithosphere along the new seismic profiles was determined by interpreting the patterns of normal and reverses magnetic anomalies extracted from the CAMP-M magnetic anomaly grid (Gaina et al., 2011). With the caveat that the magnetic data is not evenly distributed in the Eurasian Basin, and errors and uncertainties may have been introduced by data interpolation, we have interpreted the magnetic anomalies and assigned ages based on the timescale of Ogg (2012) for the chron times shown in Table 2.1.

4. Results – the Eurasia Basin tectonic structure based on new seismic data and potential field analysis

4.1. Nansen Basin

A new set of five seismic profiles cover now part of the SW Nansen Basin (ARC11-003, ARC11-004, ARC11-005, ARC11-006, ARC11-010), and one long profile (ARC14-07), extends across both Nansen and Amundsen basins and their continental margins (Figs. 1, 2). The Nansen Basin seismic profiles, together with magnetic, free air gravity, and

Table 2

1) Magnetic chrons and ages according to (Ogg, 2012) geomagnetic timescale. 2) Seafloor half spreading rates along seismic profiles presented in Figs. 5, 6, 8 and 9 (dist - is distance in km; rate is in km/myr).

Chron	Age		Geological time
	Age in Ma		
5n.1ny	9.786		
5n.2no	11.056		
6no	19.722		
13ny	33.157		Base of Rupelian
18no	40.145		Base of Bartonian
20no	43.432		
21ny	45.724		
21no	47.349		
22no	49.344		Base of Lutetian
24n.3no	53.983		

Profile number	COB-C24no (c. 3.12 myr)		C24no-C21no (6.6 myr)		C21no-C20no (3.9 myr)		C20no-C13ny (10,3 myr)		C13ny-C6no (13,4 myr)		C6no-C5ny (9,9 myr)		C13ny-C5ny (23,3 myr)	
	Dist	Dist	Rate	Dist	Rate	Dist	Rate	Dist	Rate	Dist	Rate	Dist	Rate	
11-003	58	80	12.12	32	8.2	63	6.12	x	x					
11-004	50	78	11.81	33	8.46	65	6.31	x	x					
11-005	63	82	12.42	30	7.7	61	5.92	x	x					
11-006	57	71	10.75	32	8.2	76	7.38	x	x					
11-010	x	x		x		70	6.8	55	4.1	32		77	3.3	
14-P07-A		73.34	11.11	43.5	11.15	57	5.53					72.28	3.1	
14-P07-N		80	12.12	33	8.46	78	7.57					119	5.1	
11-035		60.6	9.18	58	14.87	35	3.4	x						
11-034		82	12.42	36	9.23	53	5.15	x						
11-032		89	13.49	x		59	5.73	13	0.97					
11-031		95	14.40	30	7.69	x		x						
11-030		98	14.85	35	8.97	52	5.05	14	1.04					
11-029	18	76	11.51	24	6.15	48	4.66	12		24		57.7	2.48	
11-028	20	87	13.18	24	6.15	43	4.17	12		x		x		
11-027	16	85	12.88	23	5.9	44	4.27	12		x		51.98	2.23	
11-026		x		20	5.12	55	5.34	14		27		x		
11-024		x		x		47	4.56	11		11		x		
14-05												61.9	2.66	

bathymetry data extracted along the same profiles, are presented in Figs. 5 and 6 (un-interpreted seismic profiles are shown in Figs. S1, S2).

A distinct continent– ocean boundary (COB) is most of the time an abstract, 2D representation of a more complex, 3D structure, but this boundary is often needed for plate kinematic reconstructions. In this study, the COB is regarded as the seaward limit of the continent-ocean transition (COT). We tentatively mark the COT by attempting to interpret the landward limit of “pure” oceanic crust. This is in fact the seaward limit of the ocean-continent transition zone, but in the absence of refraction data, to locate this boundary, we can only use the seismic reflection patterns indicative of oceanic crust, together with the potential field data signature.

In the following, we summarize the structure of the Nansen Basin revealed by the new seismic profiles:

1) The acoustic basement can be followed from the continental shelf into the deep basin on two (ARC11-05 and ARC11-06) out of four profiles that cross the Barents Sea shelf into the Nansen Basin. Continental basement blocks are bounded by steep faults. Note that these two seismic profiles image the segment of the Barents Sea continental margin that has a bent and, together with its conjugate Lomonosov Ridge segment, it may have experienced strike-slip and transtensional motion during continental break-up (e.g. Minakov et al., 2012). Rugged basement topography typical for oceanic crust can be identified within a domain about 50 to 60 km south of the location where we interpreted the positive magnetic anomaly C24no (53.98 Ma).

2) The interpreted basement topography younger than C20o (43.43 Ma) is more rugged and shallower than the crust of 43 Ma and older. This is best observed on profiles ARC11-003, ARC11-004 and ARC11-005 (Fig. 5). A prominent step in the basement topography is observed around C13 old (c. 33 Ma) oceanic lithosphere, which probably marks a change in the spreading regime. A sharp transition between deep and shallow (with about 0.5 s) basement is best seen on profiles ARC11-003, ARC11-004 and ARC11-005, Fig. 5 and on profile ARC14-07, Fig. 6.

3) On line ARC11-006, the sediment package dated 45 Ma and older is deformed indicating a post-45 Ma event that disturbed it.

An additional seismic line (PGS-GWL-006), across St. Anna Trough and the Kara Sea shelf, documents break-up/post-breakup sedimentation (Fig. 7). Possible Eocene deposits lay on Paleozoic sedimentary sequences and acoustic basement. This may indicate a pre-Eocene uplift and erosion of the continental margin during break-up and incipient sea-floor spreading.

4.2. Amundsen Basin

As part of the Russian seismic data acquisition campaign presented here, many more seismic profiles have been acquired in the Amundsen Basin and adjacent Lomonosov Ridge (Fig. 1) than in the Nansen Basin. In the following we will divide the seismic data interpretation in two parts: the north Amundsen Basin (lines ARC11-035, ARC11-034, ARC11-032, ARC11-031, ARC11-030) shown in Fig. 8, and the south

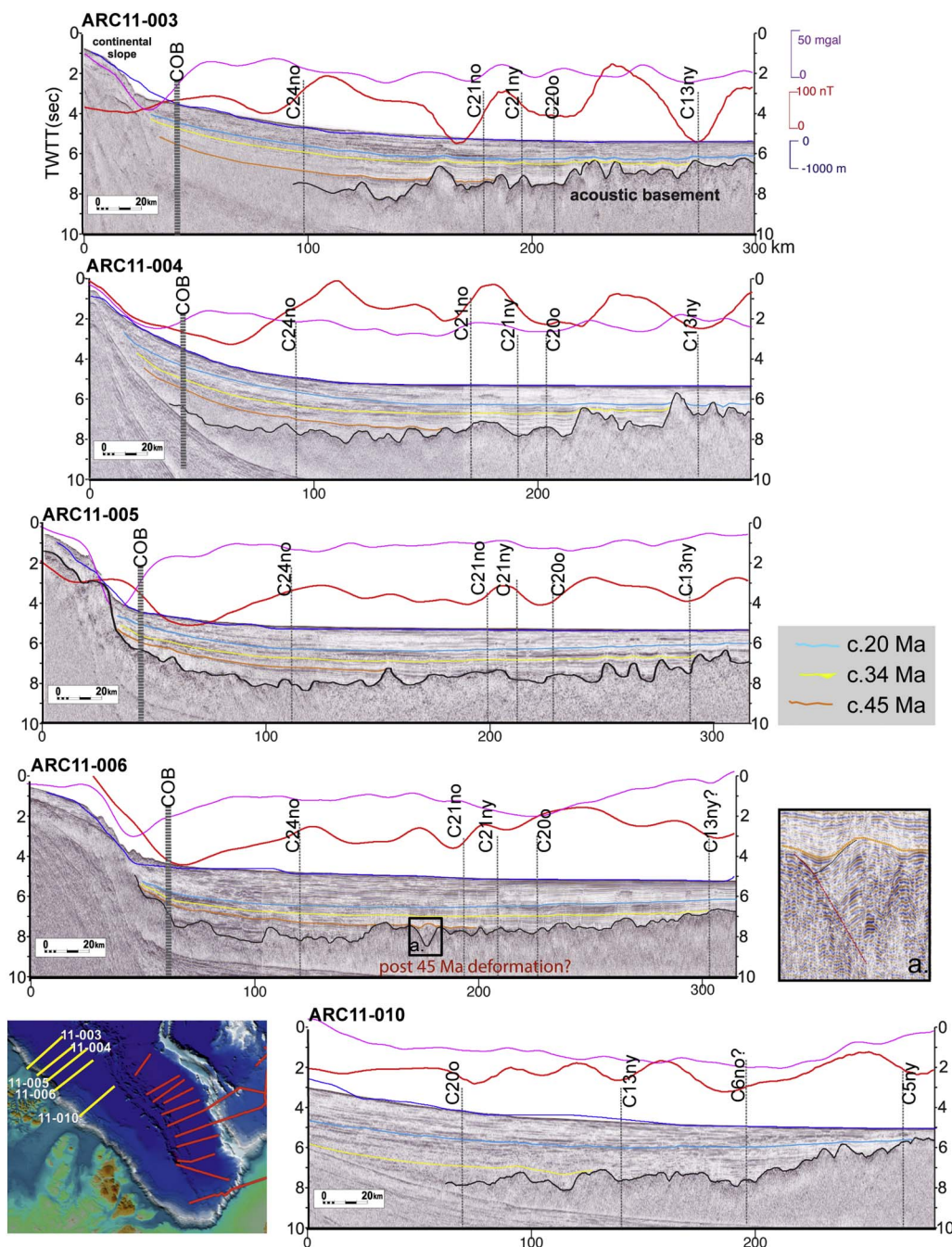


Fig. 5. Arktika-2011 (Nansen Basin) seismic profile interpretation (profile location shown in the left lower corner and in Fig. 1, un-interpreted data in Fig. S1). Magnetic anomalies (CAMP-GM, Gaina et al., 2011) along the same profiles are shown in red; free air gravity anomalies (DTU13, Andersen et al., 2014) - in magenta, and bathymetry (GEBCO2014/IBCAOV3) - in blue. “C” stands for magnetic chron. The interpreted age of seismic horizons is guided by the oceanic basement age and correlations with pan-Arctic geological and geophysical data. (For interpretation of the references to colour in this figure legend, the reader is referred to the web version of this article.)

part of the basin close to the Laptev Sea (lines ARC11-029, ARC11-028, ARC11-027, ARC11-026, ARC11-024) shown in Fig. 9. Un-interpreted seismic profiles from Amundsen Basin can be seen in Figs. S3 and S4.

From the northern Amundsen Basin seismic lines, the following observations can be noted:

- 1) The basement topography in the Amundsen Basin is much more rugged than in the conjugate Nansen Basin, as shown by numerous faulted, c. 10–20 km wide blocks (Figs. 6, 8a, b).
- 2) The first morphological change in interpreted basement topography occurs at C21 (47.33–45.68 Ma), where a prominent trough and ridge system is observed on all profiles (Fig. 8). We do observe, however, that on line ARC11-035, ARC11-034 and ARC11-032 the oceanic basement dated C22 has also a higher relief than the surrounding basement. On line ARC11-032 we can observe an unconformity in the sedimentary cover, and onlapping layers on the

C22 block, indicating tectonic uplift (Fig. 8c). On all profiles one can observe that crust younger than C21 becomes shallower.

- 3) The new seismic data document new “seamounts” or basement ridges at seafloor level which are missing in the GEBCO/IBCAO Arctic bathymetric map (see features marked with “Sm” on profiles ARC11-030 and ARC11-031, Fig. 8).

Three out of the five new S Amundsen Basin seismic lines extend to the Lomonosov Ridge margin, showing a gentle slope on lines ARC11-029 and ARC11-027, and a sharper transition to the oceanic domain on line ARC11-028 (Fig. 9). Other notable characteristics revealed by the seismic data include:

- 1) A “trough and ridge” structure divides the smoother oceanic crust older than C21 (on some lines C22), from the shallower and rougher crust c. 45 Ma and younger (Figs. 8 and 9).

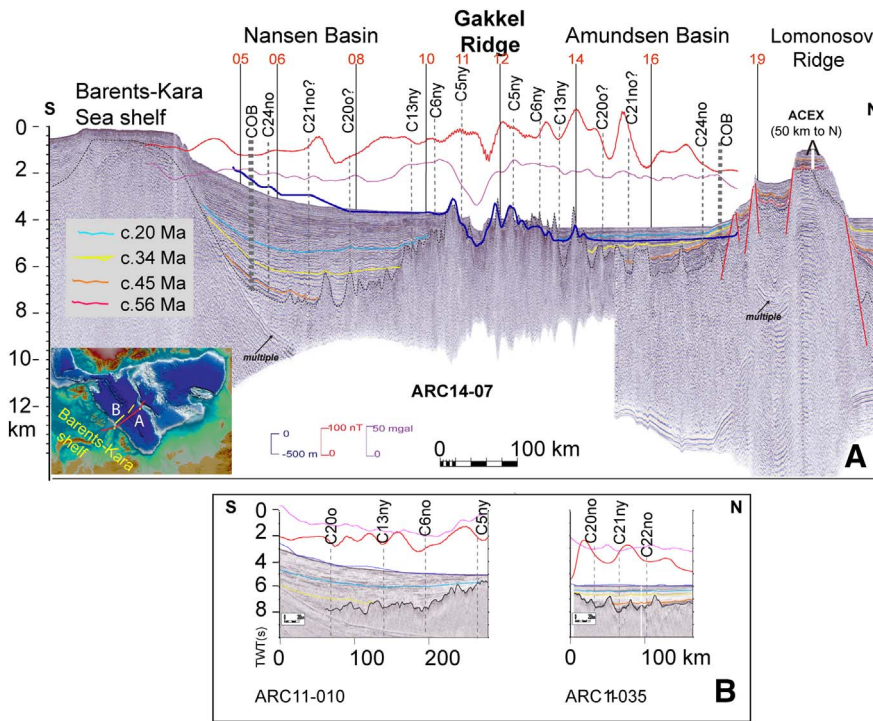


Fig. 6. A. Seismic line ARC14-07 across the entire Eurasian Basin and its continental margins (location in Fig. 1, un-interpreted data in Fig. S2), and B. Seismic lines ARC11-010 (Nansen Basin) and ARC-035 (Amundsen Basin) showing incomplete Eurasia Basin conjugate flanks. Red numbers in panel A indicate the location of sonobuoy deployments. Potential field data, bathymetric profiles, and chron interpretations as in Fig. 5. (For interpretation of the references to colour in this figure legend, the reader is referred to the web version of this article.)

- 2) A deep trough (c. 8 s two-way travel time, TWTT), with symmetrical flanks that extend for about 80 km between presumably C24no and C21no, is seen on line ARC11-027. The trough coincides with a positive magnetic anomaly peak, but is difficult to conclude whether it may be an extinct spreading ridge.
- 3) On seismic lines ARC11-024, ARC11-026 and ARC11-027 (Fig. 9), a small angular unconformity of onlap type is well seen in the sedimentary basement against oceanic crustal blocks dated C16 or C13. This unconformity traces an uplift phase that may be linked to slow/intermediate to ultra-slow spreading transition time.

4.3. Conjugate profiles in Nansen and Amundsen basins

To date, only one seismic profile continuously runs through the entire Eurasia Basin and its continental margins (line ARC14-07, Figs. 1, 6). Profiles ARC11-010 (in the Nansen Basin, Fig. 5) and ARC11-035 (in the Amundsen Basin, Fig. 9) are almost conjugate, but do not extend to the Gakkel Ridge. For a more complete picture of the Eurasia Basin conjugate flanks, we present these three profiles in Fig. 6. Note that seismic profile ARC14-07 is depth-converted, whereas ARC11-010 and 11-035 are in two-way travel time (TWTT) measured in seconds.

Profile ARC14-07 remarkably shows the asymmetry of oceanic crust accretion and sedimentation in the Eurasian Basin. Along this profile, the Nansen Basin is 360 km wide and has the deepest basement at

7.8 km, whereas the Amundsen Basin is 330 km wide with the deepest basement at 6 km. The new data suggest that the Amundsen Basin is c. 700 m shallower than shown by the GEBCO/IBCAO bathymetric grid (Fig. 6). Greater subsidence occurred in the Nansen Basin due to the higher sediment load from the Barents/Kara sea shelves; the seismic profile shows that the thickest sediment cover reaches 4 km, whereas in the Amundsen Basin is only 2 km. This observation is confirmed by the two quasi-conjugate profiles, ARC11-010 and 11-035 shown in Fig. 6B. Asymmetry is also observed in the accreted crust, with basement as old as C13 reaching the seafloor. The Amundsen Basin has rougher and shallower basement topography, with older basement (older than C20) being at almost the same depth until it reaches COB (c. 6 km). The Gakkel Ridge valley displays asymmetric flanks, with a wider and more rugged topography to the north.

4.4. Age and stratigraphy of the Eurasian Basin sedimentary cover

The age of oceanic lithosphere, as identified from magnetic data projected along the new seismic profiles, is summarized in Fig. 10. This information has been used to guide the dating of various sedimentary packages interpreted between strong reflectors in the Eurasia Basin seismic data (Figs. 5, 6, 8 and 9), and interpolated with dated sedimentary packages from the ACEX drill (Moran et al., 2006). The ACEX drill holes are about 55 km to the north of the ARC14-07 seismic profile

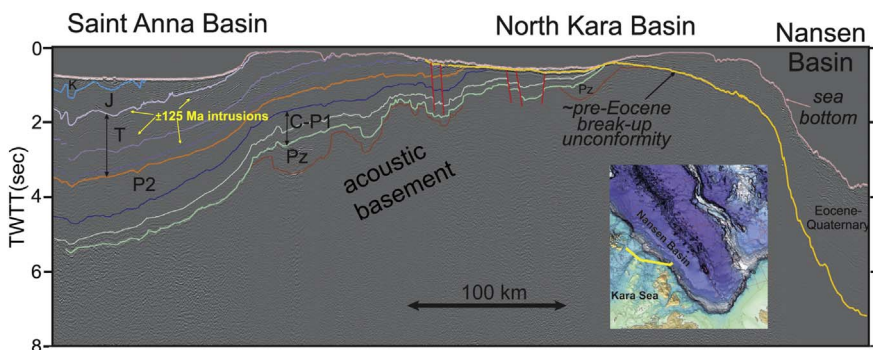


Fig. 7. Seismic profile PGS-GWL-006 interpretation along the Nansen Basin passive continental margin. The lower sedimentary cover may be Eocene strata deposited on acoustic basement and North Kara Basin Paleozoic sedimentary sequences. This indicates pre-Eocene uplift of the northern Kara margin. Profile location in inset figure and Fig. 1.

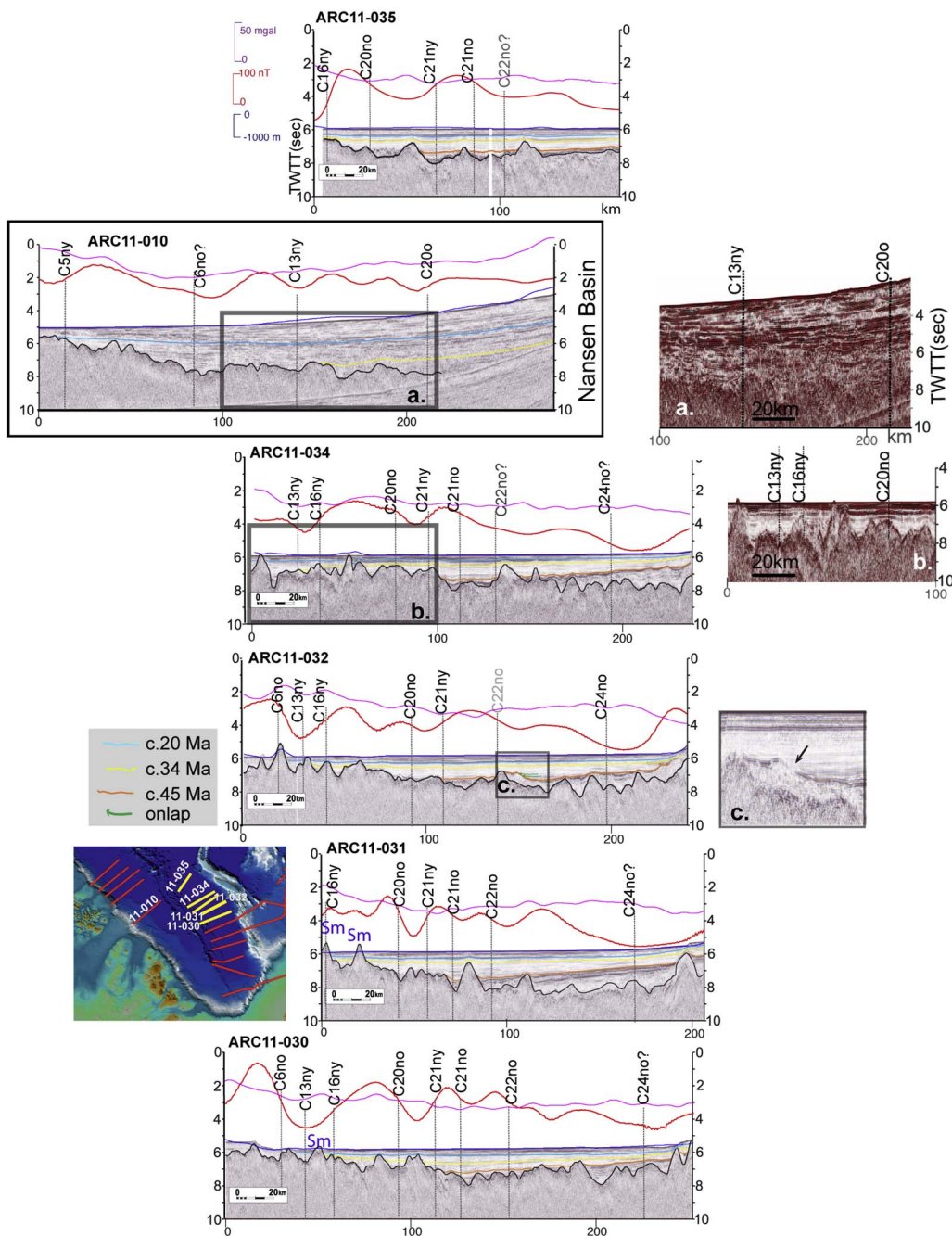


Fig. 8. Arktika-2011 (north Amundsen Basin) seismic profile interpretation (location in inset figure and Fig. 1, un-interpreted data in Fig. S3). Potential field data, bathymetric profiles, and chron interpretations as in Fig. 5. “Sm” stands for seamount.

(Figs. 2 and 6), which is imaging the same succession penetrated by the IODP drill.

We observe that the prominent seismic reflector that abuts Eurasia Basin oceanic crust formed between chrons 20no and 21no (dated 43 and 47 Ma respectively), looks very similar on seismic profiles across the Lomonosov Ridge (Fig. 6, Nikishin et al., 2014, 2017). This seismic horizon was drilled by the ACEX expedition (Moran et al., 2006) and was dated 45.4 Ma (Backman et al., 2008; Backman and Moran, 2009); consequently we assign a c. 45 Ma age to the continuation of this horizon in the Eurasia Basin. Magnetic boundary dated at 33.2 Ma is very close to the Eocene/Oligocene boundary (33.9 Ma), and therefore we propose that the seismic boundary that terminates against the C13 (33.2 Ma) oceanic ridges coincides with the Eocene-Oligocene boundary.

Following the correlation between sedimentary packages, age of oceanic lithosphere determined from the magnetic data, and dated

sedimentary succession from the ACEX drill sites, the age of the four main sedimentary packages identified in the new seismic dataset may be: (1) Early to Mid Eocene (c. 56 to 45.7 Ma), (2) Mid Eocene to Early Oligocene (45.7 to 33.2 Ma), (3) Early Oligocene to Early Miocene (close to Aquitanian) (33.2 to 19.7), and (4) Early Miocene (close to Burdigalian) to Present (19.7 to 0 Ma).

As part of the new Russian geophysical dataset, several seismic profiles run along the Lomonosov Ridge and its slopes towards the Amundsen Basin (Fig. 1). On these profiles we see a rift-postrift type boundary and suggest that it corresponds to the break-up boundary, marking the onset of the Eurasia Basin opening (Nikishin et al., 2014, 2017; Gaina et al., 2015). We note that this boundary was also identified within the Laptev Sea (Franke, 2013; Khoroshilova et al., 2014; Nikishin et al., 2014; Weigelt et al., 2014), and we consider it of Paleocene-Eocene or early Eocene age. A slightly younger horizon is imaged on the seismic line that crosses the Kara Shelf continental margin

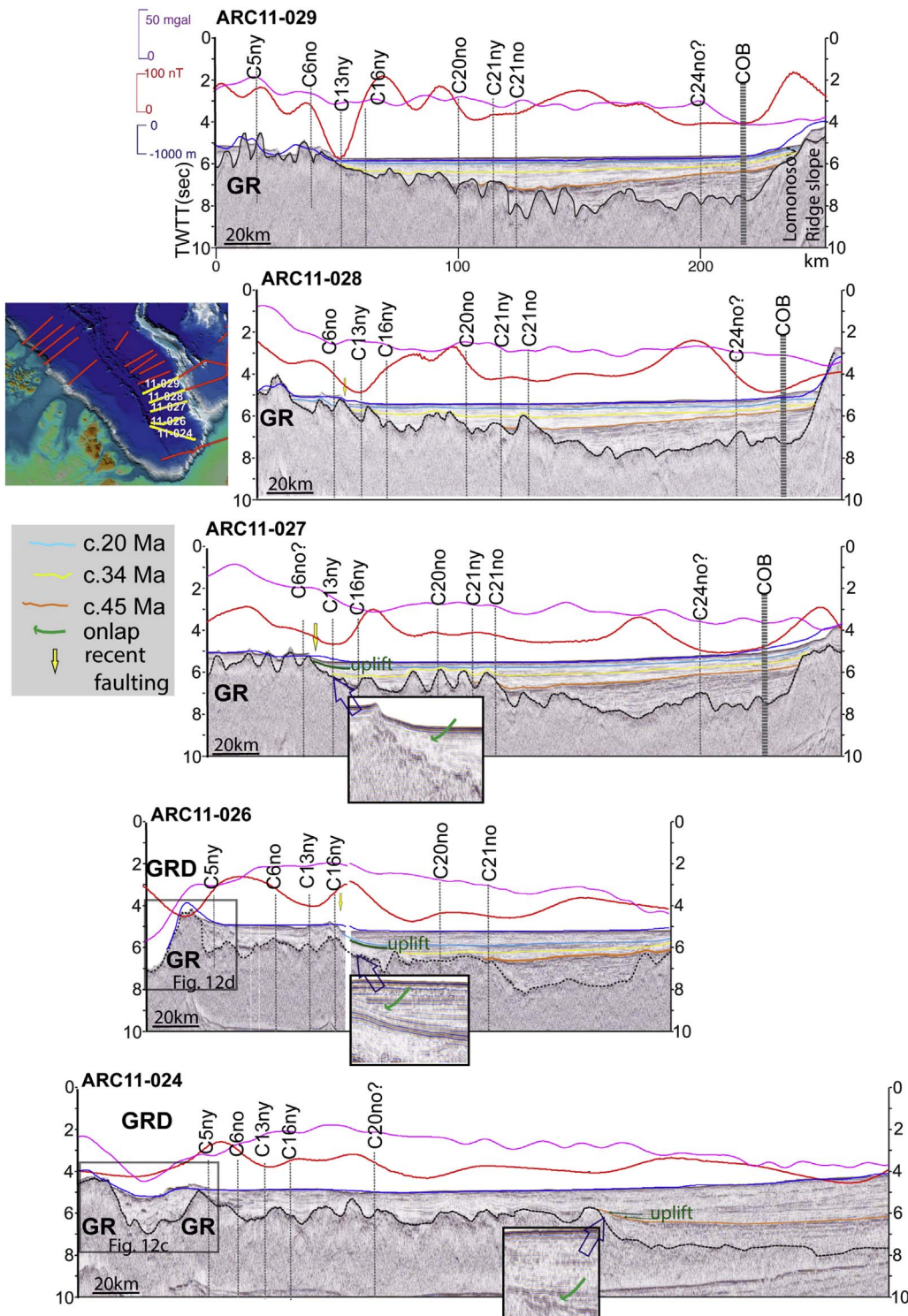


Fig. 9. Arktika-2011 (south Amundsen Basin) seismic profile interpretation (location in inset figure and Fig. 1, un-interpreted data in Fig. S4). GR stands for Gakkel Ridge, GRD is the Gakkel Ridge Deep, see sections 4.5 and 4.6. Potential field data, bathymetric profiles, and chron interpretations as in Fig. 5.

(Fig. 7). This sedimentary horizon covers underlying deposits with an angular unconformity, probably linked to continental break-up, and therefore also of early Eocene age (Fig. 7).

4.5. Gakkel Ridge

The complete rift valley and conjugate elevated flanks of the Gakkel Ridge (Figs. 11, S5) are imaged by two seismic profiles oriented perpendicular to the ridge (Fig. 1). Profile ARC14-07 (Fig. 6 and 11A) shows the mid-ocean ridge structure in the central Eurasia Basin, and

profile ARC14-05 (Fig. 11) is documenting the configuration of the easternmost part of the basin, a region poorly mapped by seismic data until now.

The Gakkel Ridge basement shown by the seismic profiles in Fig. 11A, B, is characterized by a rough trough-and-ridge topography with normal faults (marked by red lines), uplifted rift shoulders, rotated blocks and syn-rift sediments. Such steep faults have been described in the Knipovich Ridge region, an area of ultra-slow seafloor spreading (e.g. Kvarven et al., 2014). Gakkel Ridge rift shoulder uplift seems to be synchronous with tectonic block rotation (Fig. 11A, B).

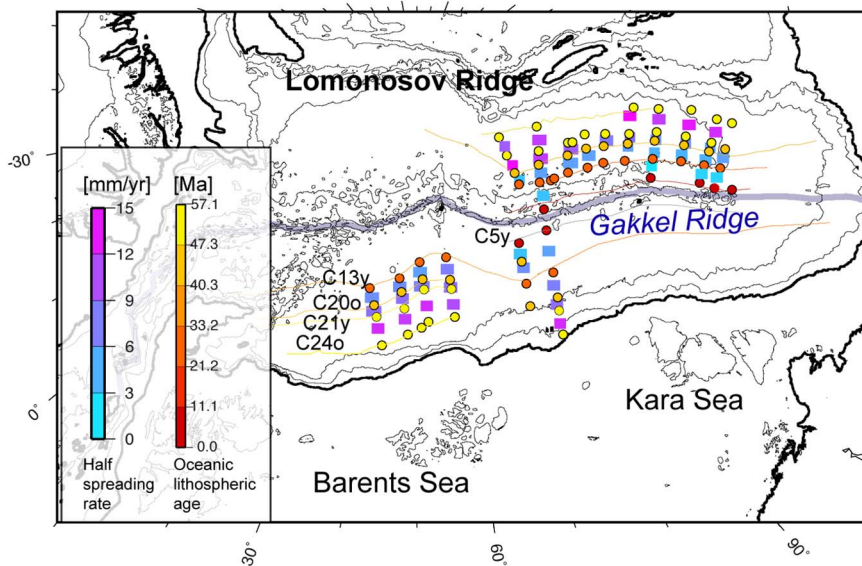


Fig. 10. Magnetic anomaly identifications and seafloor half spreading rates calculated according to the new oceanic lithosphere age identifications along the seismic profiles shown in Figs. 5, 6, 8 and 9 (see also Table 2).

The Gakkel Ridge and recently formed valley in the central Eurasian Basin are asymmetric, with about 80 km wide elevated topography (c. 3500–4000 m) in the Amundsen Basin, compared to only 50–60 km wide high ridge topography in the Nansen Basin (Fig. 6 and 11A). This asymmetry is also observed in the eastern Eurasia Basin, where the Gakkel Ridge forms at the slowest pace (Table 2.2 and Fig. 10), with rift shoulders c. 50 km wide (in the Nansen Basin), versus c. 70 km wide in the Nansen Basin (Fig. 11). The general Gakkel Ridge asymmetry is reflected in the bathymetry and potential field data (gravity and magnetics, Figs. 2, 6, 11). Negative free air gravity values indicate that the ridge is magma starved, or the magma chamber is very deep. The Gakkel Ridge valley is characterized by a broad (in its central part, Fig. 11A), or narrower (in the eastern part, Fig. 11B), positive magnetic anomaly showing the formation of oceanic crust from chron C1 normal (Brunhes, 0.78 Ma) at a depth of approximately 3.5 km.

4.6. The Gakkel Ridge Deep

The new seismic data document for the first time the deepest valley along the Gakkel Ridge, a deep basement structure situated very close to the easternmost tip of the Gakkel Ridge (Fig. 11B). For an easy reference, we will call this deep-graben: the **Gakkel Ridge Deep** (GRD).

GRD has been detected by earlier Russian bathymetric charts and imaged by modern bathymetric maps (IBCAO v3, Jakobsson et al., 2012), which incorporated information from those charts. The Russian new seismic data allow now mapping this feature in greater detail. GRD is surrounded by steep faulted blocks, which may have been overprinted by volcanic edifices in several places (Fig. 12). In its deepest part (c. 5200 m), the GRD is about 95 km long and 30–45 km wide, and the basin's depth relative to the shoulder uplifts is 1800–2000 m. The seismic line ARC11–026 crosses the Shaykin seamount situated on the elevated GRD rim (Fig. 12); a feature registered by the GEBCO Gazetteer as the “Shaykin Hill” named by the Russian scientist G. Grikurov in 2003. GRD elevated bathymetric flanks may host volcanic edifices shown by the seismic reflection data as pointed hills features (Fig. 12). One of this “pointy hill” is seen in the multibeam high-resolution bathymetric data collected along the ARC14–05 seismic line (Fig. 12A), and a detailed topographic image suggests a seamount-like feature with rugged eastern flanks (Fig. 12B.e.). Strong reflectors indicating volcanic material are seen within young sediments accumulated in the GRD adjacent rift valley (Fig. 12). Note that the northern GRD flank displays a prominent circular magnetic anomaly, and two smaller similar anomalies are seen within the deep part of GRD (Fig. 12A), indicating a

magmatic origin of these features. Very recent, Piskarev and Elkina (2017) postulated that this Gakkel Ridge segment hosts a giant caldera that erupted 1.1 myr ago, and spewed volcanic material as far as 1000 km away.

The seismic line ARC14–20 (Fig. 11) runs along the GRD eastern edge, and further southwards is parallel to the GRD's valley. South of GRD, the next Gakkel Ridge segment is limited by a large seamount (Fig. 11), which we call the Trubyatchinsky Seamount to honor the 2014 expedition vessel name (*Nikolay Trubyatchinsky*). In its tectonic position, the Trubyatchinsky Seamount is similar to the Logachev Seamount of volcanic origin (Okino et al., 2002; Schindwein and Schmid, 2016), which separates different segments of the Knipovich Ridge rift valley (Jokat et al., 2012), and illustrates that considerable volcanic activity is occurring on ultraslow spreading ridges as also mentioned by previous studies (e.g. Sohn et al., 2008).

5. Discussions

5.1. Seafloor spreading asymmetry in the Eurasia Basin

Oceanic seafloor spreading process is characterized as “symmetric” if, for a particular time period, the same amount of oceanic lithosphere is accreted on conjugate flanks. A global study shows that seafloor spreading created asymmetric lithospheric flanks in many oceanic basins worldwide (Müller et al., 2008), mainly in regions where mantle thermal anomalies facilitated ridge jumps and oceanic lithosphere transfer from one flank to another.

It has long been observed and reported that the Nansen Basin is shallower than the Amundsen Basin, due to the thick sediment load accumulated in the former from the Barents and Kara sea continental shelf erosion (e.g. Jokat et al., 1995). North of Barents and Kara seas continental margins, one can identify a deeper “top of oceanic basement” than adjacent to the submerged Lomonosov Ridge margin (Fig. 6). Besides this depth asymmetry, earlier geophysical data also revealed an asymmetry in oceanic lithosphere accretion in the two Eurasia sub-basins. Among the first to report asymmetry in the seafloor spreading based on magnetic anomaly data, Vogt et al. (1979) described an asymmetry for younger crust (up to C6), and suggested that the asymmetry is increasing for older crust, with half spreading rates in the Amundsen Basin consistently lower (with 10–20%) than in the Nansen Basin. Jokat and Micksch (2004) used modern multichannel seismic profiles in the western Nansen and Amundsen basins (acquired in 2001 with the German and US icebreakers RV Polarstern and USCGC

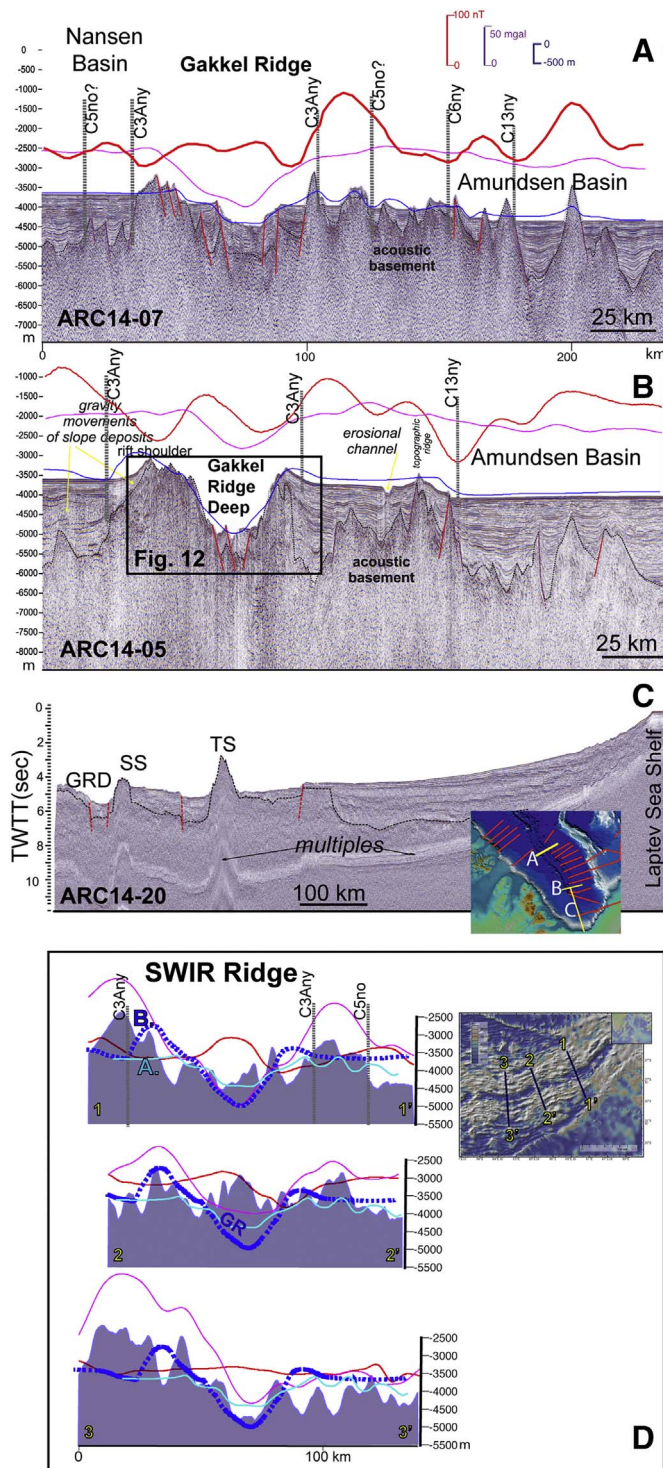


Fig. 11. Interpretation of seismic profiles across the Gakkel Rift valley, and comparison with selected Southwest Indian Ridge bathymetric profiles (location in inset figure and Fig. 1, un-interpreted data in Fig. S5). A is a fragment of seismic profile ARC 14-07 (see Fig. 5A), B is a fragment of seismic profile ARC 14-05 (Fig. 1), and C is seismic profile ARC 14-20. Red solid lines are possible normal faults. Abbreviations: GRD - Gakkel Ridge Deep, SC - Shaykin seamount, TS - Trubyutchinsky seamount. C. Bathymetry (GEBCO2014), magnetic anomalies (WDMAM) and free air gravity (DTU13, Andersen et al., 2014) along selected profiles across the Southwest Indian Ridge (SWIR); see profile location on the right hand side. Cyan profile and blue thick dotted line are segments of the Gakkel Ridge bathymetric profiles shown in panel A and B, respectively, plotted at the same scale with the SWIR bathymetry. (For interpretation of the references to colour in this figure legend, the reader is referred to the web version of this article.)

Healy) to explore the characteristics of oceanic crust and sedimentary cover. Although the analysed profiles are not conjugate, Jokat and Micksch (2004) noticed the much rougher basement topography of the Amundsen Basin flank, and also a sharp decrease in basement depth between chrons 12 and 18 on the same flank. Jokat and Micksch (2004) concluded, based on the two seismic profiles in the west Eurasia Basin and an analysis of basement subsidence vs. spreading rates, that the spreading regimes in the two sub-basins were offset, with the Amundsen Basin meeting a slower regime much earlier than in the Nansen Basin, and hence the difference in basement topography on the two flanks.

We have used the newly interpreted magnetic chrons and location of continent-ocean boundary (Figs. 5, 6, 8, 9 and 10), to evaluate the seafloor spreading rates along the seismic profiles in the Nansen and Amundsen basins, and computed median values for several time intervals (Table 2.2). The result of our calculation has been added on Fig. 10. As reported by many other studies before, following break-up, the Eurasia Basin first opened at intermediate rates (e.g. Glebovsky et al., 2006; Vogt et al., 1979). We note that a 50–60 km region with negative magnetization, that marks the first oceanic crust probably dated C24r (53.98–57.1 Ma), formed at a median half spreading rate of 17.5 km/myr, which is 150% higher than the highest seafloor spreading rate computed for younger times based on this study data (see Table 2.2).

This new seismic dataset documents for the first time a complete, conjugate transect through the entire eastern Eurasian Basin and its margins (Fig. 6), and therefore allows a proper quantitative analysis of observed asymmetry in oceanic lithosphere accretion on conjugate flanks. The seafloor spreading rates calculated along this long profile (Table 2.2 and Fig. 10) show higher values in the Nansen Basin than in the Amundsen Basin except for the spreading stage C21no–C20no (c. 47–43 Ma), when the report is reversed. At this time, the second peak of the deformation between north Greenland and Lomonosov Ridge/southern Eurasia Basin, known as the Eurekan orogeny or deformation, could have affected a larger portion of the Arctic as suggested by Gaina et al. (2015). A prominent change in the sedimentation pattern is also dated at c. 45 Ma (e.g. Backman and Moran, 2009), and is visible on all our seismic profiles. We note that the ARC14–07 profile aligns with the Lomonosov Ridge structural bend (Fig. 6), which may represent an important tectonic boundary (e.g. Minakov et al., 2012; Shipilov and Vernikovskiy, 2010), whose location may have influenced at least the early seafloor spreading evolution. This configuration is probably inherited from a pre-breakup basement configuration that places a suture (Caledonian or Timanian), and associated orogenic tectonic grain, perpendicular to the Eurasia Basin southern margin (Figs. 3 and 13). We suggest that the reversal in the oceanic crust asymmetry and subsequent ultraslow spreading rates (Table 2.2 and Fig. 10) could have been triggered by a series of plate boundary re-adjustments due to either competing tectonic stresses or different rheology in surrounding tectonic environment.

5.2. Eastern Gakkel Ridge and SWIR

The structure of the western Gakkel Ridge - a part of plate boundary between Eurasia and North America, and the rules of plate tectonics, indicate that this mid-ocean ridge falls under the ultra-slow spreading ridges category. Similar seafloor spreading regimes are found only in few places on Earth (e.g. Dick et al., 2003; Snow and Edmonds, 2007; Kandilarov et al., 2010), and the Southwest Indian Ridge (SWIR) is probably the closest analogue to the GR, although SWIR is much farther away from continental margins than GR. Since the eastern Gakkel Ridge has been poorly surveyed so far, we firstly analyse its geomorphology and compare it with known ultra-slow spreading mid-ocean ridge structure. A comparison between the GR and SWIR structures is shown in Fig. 11C. Three profiles documenting the SWIR configuration for a segment situated close to its northeastern tip at the Rodriguez Triple

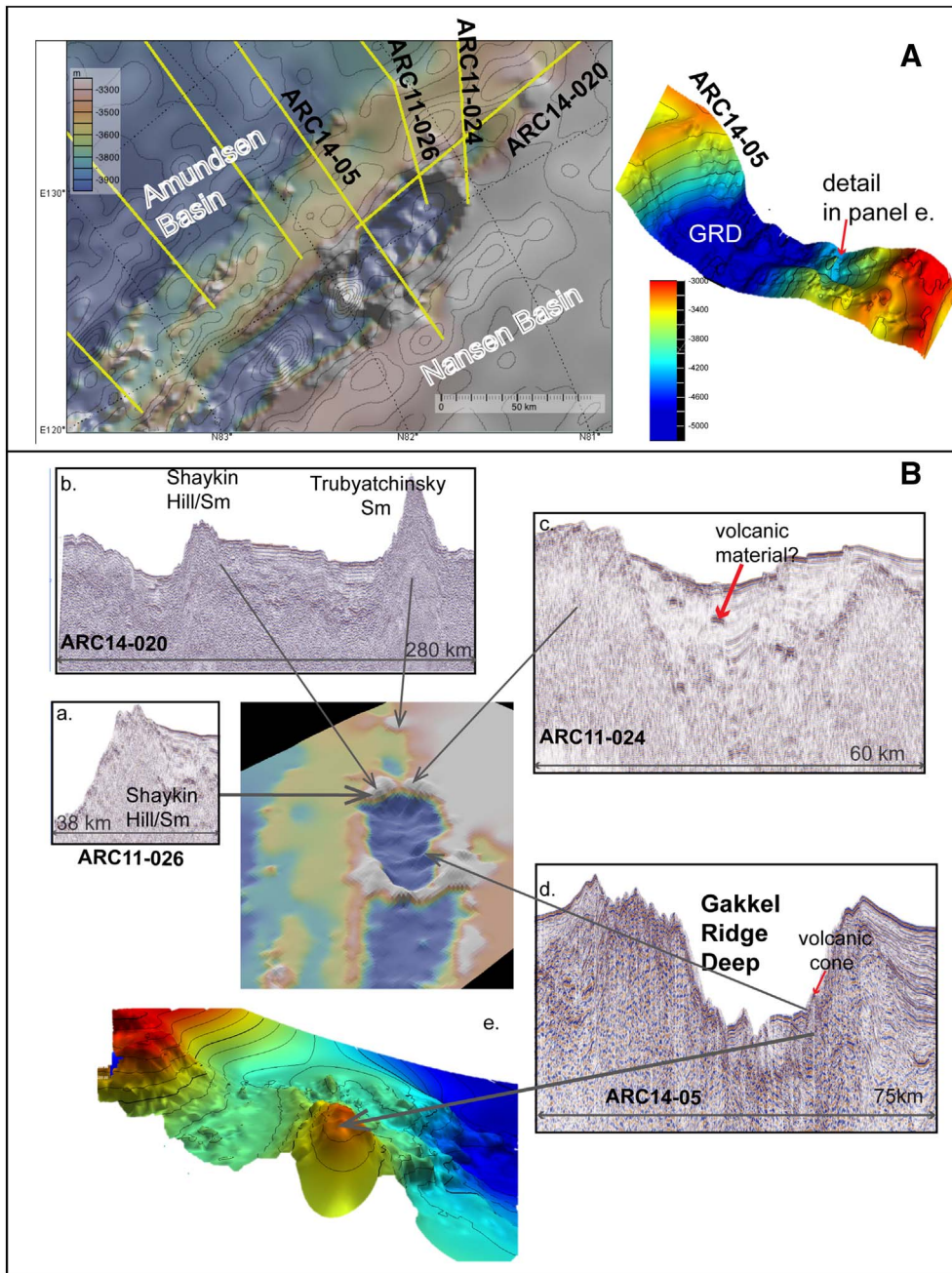


Fig. 12. The Gakkel Ridge Deep. A. Bathymetry (IBCAO v3, 500 m grid resolution) and contours from magnetic anomaly grid CAMP-GM (Gaina et al., 2011). Yellow lines are seismic profiles discussed in this study. B. 3D image of bathymetry (same as in A.), and detailed images of seismic data showing volcanic constructs within GRD and on its flanks. Panel e shows gridded multibeam data (90 m cell size) collected along ARC14-05 profile. (For interpretation of the references to colour in this figure legend, the reader is referred to the web version of this article.)

Junction, show a transition from a deep valley (c. 4000 m) with asymmetric ridge flanks (profile 3–3', Fig. 11C), to a region where an elevated block (at 3000 m depth) occupies the central mid-valley, and where the ridge flanks are more symmetric (profile 2–2', Fig. 11C). From there, the ridge is continuing towards a broader central valley where a more recent rift has been developed within an older structure, with asymmetric rift shoulders (profile 1–1', Fig. 11C). The GR bathymetric profiles from central (Fig. 11A), and eastern (Fig. 11B) part, are superimposed at the same scale on the SWIR bathymetry along the three profiles (Fig. 11C). The morphology of GR in its central part resembles well with the asymmetric, central SWIR segment. The narrower, GR “double” rift valley (or an incipient volcanic construction within older axial ridges), situated at its slowest spreading part (shown in Fig. 11B), matches well the ultra-slow SWIR segment nearby the triple junction (and therefore closest to the rotation pole). Both SWIR and Gakkel Ridge display asymmetric rift shoulders in their respective segments close to the rotation poles (Fig. 11C, profile 1–1').

Mendel et al. (2003) described the morphology of various SWIR segments based on detailed multibeam data. They conclude that the asymmetry of SWIR abyssal hills reflect the oceanic crustal thickness and its tectono-magmatic history. Larger abyssal hills are connected to thicker crust formation, whereas smaller abyssal hills are found in regions of thinner crust, thus reflecting the amount of magma supply. As in the SWIR case, we also observe that the GR flanks with shallower and rugged structure are more regularly spaced (Fig. 11A right hand side), and this may indicate periodic tectonic phases, as suggested by Mendel et al. (2003).

5.3. Along-ridge segmentation of the eastern Gakkel Ridge valley

Along-ridge segmentation of the western Gakkel Rift was observed in bathymetry, gravity, and magnetic signals, was revealed by local seismicity, and by the petrology of rock samples collected from rift valley (Michael et al., 2003; Jokat et al., 2003; Schmidt-Aursch and

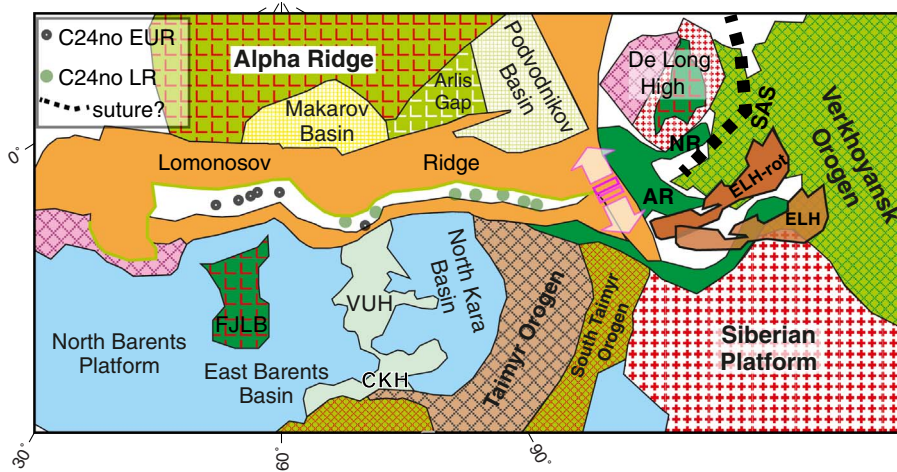


Fig. 13. Main tectonic provinces flanking Eurasia Basin (as in Fig. 3) reconstructed at C24no time (53.98 Ma). Barents/Kara seas and Lomonosov Ridge continental margin outlines have been adjusted according to the COB (continent-ocean boundary) interpretation shown in Figs. 5, 6, 8 and 9. Magnetic picks for C24no shown in green and grey. ELH is East Laptev Horst shown in two positions: semi-transparent polygon shows ELH location in the absence of Paleocene rifting in the East Laptev Sea rift system; the brown polygon shows the rotated ELH to account for rifting that may have occurred prior to Eurasia-North America break-up. Abbreviations: AR-Anisim Rift depocenter, CKH-Central Kara High, FJL-Franz Josef Land, NR-Novosibirsk rift depocenter, SAS-South Anyui Suture, VUH-Vize-Ushakov High. (For interpretation of the references to colour in this figure legend, the reader is referred to the web version of this article.)

Jokat, 2016; Schlindwein and Schmid, 2016). The segmentation is not defined by transform faults, as in most mid-ocean ridges, but in the morphology of the ridge determined by the magma supply. On this basis, the segments were labeled “magmatic” and “sparsely magmatic/amagmatic” (e.g. Michael et al., 2003). This segmentation has been mostly described for Gakkel Ridge up to 85°E longitude - the most easterly point reached by the AMORE expedition (e.g. Michael et al., 2003). More recent studies have investigated microseismicity of a confined portions of the Gakkel Ridge at 85°E, as discussed for example by Korger and Schlindwein (2014). Here we briefly discuss the eastern Gakkel Ridge (longitude 60 to c. 123°E) segmentation, based on the most recent gridded gravity data (DTU 13, Andersen et al., 2014), recorded seismicity, and on the new Russian seismic reflection data.

Engen et al. (2002) divided the Gakkel Ridge in many segments according to the type of seismicity displayed by 1959 to 1999 earthquakes. According to that study, east of the 60°E Gakkel Ridge “bend”, a large segment (c. 370 km) displays intense seismicity and extensional faulting. East of that region, Engen et al. (2002) interpret another three similar, albeit shorter, extensional segments, which are intercalated with areas where strike-slip or oblique motion is predominant. The new free air gravity data (DTU13, Andersen et al., 2014), and seismic events recorded from 1960 to 2016 (Fig. 14), indicate that the first order segmentation of the eastern Gakkel Ridge may be described as four segments with intense seismic activity (A1-A4 indicated with grey ellipses in Fig. 14), of which the westernmost one is the most active, and three regions with less seismic activity (I1-I3). The ridge flanks of A1-

A4 display higher gravity anomaly values compared to I1-I3. The A1 region shows the highest number of earthquakes along the ridge (including a zone of swarm earthquakes < 30 km deep, according to the ISC + EMSC earthquake catalogues from 1960 to 2016), with the latest larger earthquake (magnitude 4.7) registered on 22.10.2016 (shown with magenta star symbol in Fig. 14). Another cluster of earthquakes aligns perpendicular to the ridge, at a location that coincides with a change in the Gakkel Ridge spreading direction (a “kink”) at 86°E longitude (blue ellipse in Fig. 14).

Seismic line ARC 14-07 crosses the A1 region, documenting for the first time the structure of the Gakkel Ridge east of 85°E longitude. As discussed in a previous section (see Fig. 11), a cross-section through the Gakkel Ridge and valley shows 3200–3500 m deep, asymmetric flanks, with a higher and rounded peak in the Amundsen Basin that resembles a volcano (tentatively interpreted by us as C3Any old), and a faulted ridge valley which is c. 50 km wide and 4200 m deep (Fig. 11). The entire A1 region exhibits wide ridge flanks with high free air gravity anomaly values in the Amundsen Basin (Fig. 14). Region A2 has a more symmetric structure with features that resembles seamounts on both sides of the Gakkel Ridge (magenta ellipses in Fig. 14 indicate features with high bathymetry and gravity anomaly values). The new seismic lines stop shortly before encountering the Gakkel Ridge high topography (Fig. 8), but they imaged three undetected seamounts (“Sm” in Fig. 8), located in a seismically active off-axis area, which may be connected to recent volcanic activity. A3 is a c. 400 km long “active” segment of the Gakkel Ridge defined by relatively high seismic activity

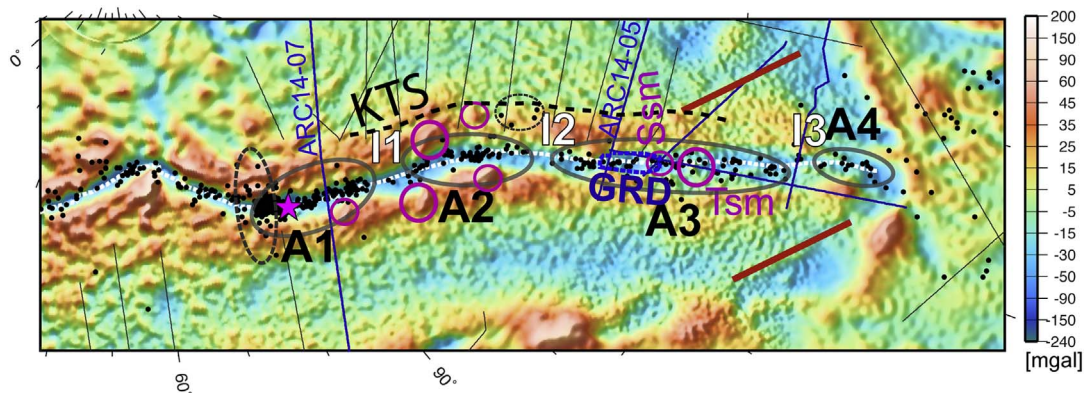


Fig. 14. Along-ridge segmentation of East Gakkel Ridge. Background: free air gravity anomaly (DTU13, Andersen et al., 2014). Thin grey lines show the location of seismic profile presented in the text, blue lines are profiles running through the Gakkel Ridge central valley. Black dots are location of earthquakes (1959–2015) with magnitude > 4 from the ISC catalogue (<http://www.isc.ac.uk>). Magenta star shows the location of recent (2016) magnitude 4.7 earthquake. A1-A4 grey ellipses indicate Gakkel Ridge “magmatic” segments which are divided by I1-I3 “amagmatic or sparsely magmatic” zones. Interpreted volcanoes/seamounts are indicated by magenta circles. The easternmost Gakkel Ridge location at pre-Late Eocene time is shown by red lines, as suggested by Gaina et al. (2015). KTS is Kazmin Tectonic Scarp, GRD is Gakkel Ridge Deep, Ssm is Shaykin seamount, Tsm is Trubyutchinsky Seamount. (For interpretation of the references to colour in this figure legend, the reader is referred to the web version of this article.)

(although lower than in A1 and A2 segments previously described). This segment starts just west of the GR deepest segment (GRD, Figs. 11 and 12), and continues almost to the easternmost tip of the Gakkel Ridge (although a less seismically active zone may divide this region in three parts, see Fig. 14).

In the southern Amundsen Basin towards the Laptev Sea, sediments younger than Miocene (c. 33–20 Ma) seem to onlap on the newly formed bathymetry, indicating vertical motion of the Gakkel Ridge (Fig. 9). The bathymetric scarp that coincides with this boundary is called in this study the “Kazmin Tectonic Scarp” (after Yury Kazmin - the scientific head of Russian Federal Arctic project who planned the seismic acquisition). Vertical motion of ultra-slow spreading ridges due to intense tectonic activity and serpentinisation that results in a more buoyant crust, has been described for the Knipovich Ridge (North Atlantic) and SWIR (Indian Ocean), and we suggest that these processes may also explain the formation of the Kazmin Tectonic Scarp (KTS, Fig.14).

The easternmost Gakkel rift valley is filled with sediments, and this observation led some authors to postulate that the ridge is an old feature, as an explanation for a sediment-filled area which is situated relatively far from continental sediment sources (Rekant and Gusev, 2016). In the c. 5200 m deep GRD, probably the deepest rift valleys in the Gakkel system, sediment thickness is about 300–500 m, while in the rift segment east of the GRD, the sediment thickness exceeds 1000 m (see Figs. 9, 11, 15). Asymmetric rift flank topography and its dynamics may be the reason for different sedimentation patterns within the rift valley.

5.4. Transition from oceanic to continental domain in the easternmost Eurasia Basin

In the area where the Gakkel Ridge approaches the Laptev Sea Shelf, the ridge is buried under sediments, and has a very faint signature in the seabed topography (Figs. 1, 2), but is relatively well imaged by the free air gravity anomaly (Figs. 2, 11), and magnetic anomaly (Fig. 2). On the seismic data, we can see the easternmost GR segment at 78.8° N, just before becoming an intra-continental plate boundary (Figs. 15, S6). The buried valley (to 6.6 s TWTT) is flanked by steep and high (to 4 s TWTT) flanks, and is characterized by negative magnetic and gravity anomalies. Recent small-amplitude normal faults that disturb Quaternary sediments, indicate recent tectonic activity (Fig. 15, profile AB). From this point imaged by the seismic data, up to the Laptev Sea shelf, the recent structure of the Gakkel Ridge is seen as a gravity low that turns to the west with a small offset (c. 60 km), as also indicated by recent, and very high seismicity (Fig. 15 lower panels). These evidences confirm that the mid-ocean ridge is continuing until it abuts against the continental shelf, as also suggested by Sekretov (2002), based on of the first seismic profiles for that region.

From the tip of the Eurasia Basin, the plate boundary shifts to the east along a small segment of transfer fault called “Severnnyi transfer” by Fujita et al. (1990). This boundary aligns with a small circle projected around the recent pole of opening between the North American and Eurasian plates (e.g. 60.32° N, 140.40° E; Merkouriev and DeMets, 2014), and was detected also by older seismic reflection data (e.g. Franke et al., 2001). This small transfer-segment links the mid-ocean ridge to the intra-continental plate boundary that follows the trend shown by smaller and intermediate earthquakes (Fig. 15 lower panels). Positive magnetic anomaly and gravity peaks characterize a c. 35 km wide region, where deformed upper sedimentary layers (Fig. 15 profile A'B') indicate recent tectonic activity. This region constitutes the northernmost part of the plate boundary in the Laptev Sea. Note that a much-reduced cluster of seismic events is located also to the west of the presumably recent plate boundary, indicating a larger region of deformation. The ION-11-4600 (A'B' segment shown in Fig. 15) reflects the general structure of the Laptev Sea rifts in the proximity of the Eurasia Basin southern boundary. The sedimentary packages in the

Laptev and East Siberian shelves are only dated by extrapolation from exposed island geology and regional seismic stratigraphy tied to the few wells existent in the Arctic region (e.g. Weigelt et al., 2014), although the rifting ages are still disputed (e.g. Drachev et al., 2010). According to the sediment packages succession and total sediment thickness interpretation, rifting may have migrated from east to west, from probably Cretaceous to recent times, as inferred from the sediment thickness variation shown by the seismic line ION11-4600. This interpretation contradicts the eastward rejuvenation of rifting in the northern Laptev Sea from west to east as suggested by Drachev et al. (1998).

Previous studies attempted to reconstruct the location and the type of plate boundary between the Eurasia Basin and the eastern Laptev Sea rift system. It has been postulated that a transform fault trending orthogonal to the Gakkel Ridge, a feature called Khatanga-Lomonosov Fault (KLF), facilitated the motion of the Lomonosov Ridge and adjacent Amundsen Basin north of the Laptev Sea (Grachev, 1983; Drachev et al., 1998, 2010; Sekretov, 2002; Franke, 2013; Pease et al., 2014; Doré et al., 2016; Nikishin et al., 2017). Recent data collected by German scientists and interpreted by Jokat and Ickrath (2015) and Jokat et al. (2013), indicate undisturbed Cenozoic sediments along a line that is crossing the NE Eurasia Basin, the Lomonosov Ridge and adjacent Podvodnikov Basin along 81° N. Based on this data, and arguing that recent seismicity at the junction between the East Siberian Shelf and the Lomonosov Ridge (the presumed termination of the KLF) is absent, Jokat et al. (2013) suggest that a transform fault between the Lomonosov Ridge and the Laptev Sea shelf may have been active only before the Eurasia Basin oceanic crust formation. Poselov et al. (2012) and Nikishin et al. (2014, 2017) interpreted new Russian seismic data (see their 7-AP profile), and concluded that a faulted basement overlain by a sedimentary cover showing a small depression above that basement fault, may be the locus of the Khatanga-Lomonosov transform.

We inspect four seismic profiles that are crossing the postulated zone of strike-slip between the Lomonosov Ridge and the Laptev Sea/Siberian Sea shelves (Figs. 16, S7). The two profiles crossing the Podvodnikov Basin and the Siberian Shelf indicate that the older sediments (Paleocene-Eocene?) were indeed disturbed (Fig. 16). The tectonic deformation observed on profile ARC14-14 was interpreted by Gaina et al. (2015) as a result of the Eureka event far-field stresses. The two profiles crossing the Amundsen Basin and terminating against the Laptev Sea shelf (ARC14-22 and ARC14-23), indicate break-up related basement faulting (Fig. 16). On line ARC14-22 we mark a basement high next to the Lomonosov ridge as “Ra” following Gaina et al. (2015), who suggested that this block formation marks a seafloor spreading re-orientation due to the Eureka-related compression in the Eocene. An elevated basement block of unknown origin (“?” on profile ARC14-22 in Fig. 16) is connecting the Amundsen oceanic basin and the continental tilted blocks of the Laptev Sea shelf.

In order to get a first order indication of the plate boundary continuation from Eurasia Basin into the Laptev Sea shelf at the time of continental breakup and first seafloor spreading, we have reconstructed the main geological provinces shown in Fig. 3 at the C24no time (53.98 Ma), by using a slightly modified Gaina et al. (2002) rotation (latitude = 62.5° N, longitude = 143.47° N, and angle = -12.89). The reconstruction makes the simple assumption that the Eurasia Basin and its southern margin belongs to the Eurasian plate, whereas the Lomonosov Ridge and adjacent Amerasia Basin, East Siberian Shelf and eastern Laptev Sea rift system were attached to the North American plate, at least since the Paleogene. According to this model, continental break-up and early seafloor spreading followed an orientation along the northward projection of the South Anyui suture (SAS), between the Anisin and Novosibirsk rift complexes (Fig. 13).

Reconstructions of the Eurasia Basin and Laptev Sea region for selected times during the Eocene to Present by using the same assumptions as above and rotations from Gaina et al. (2002) adjusted to the Ogg (2012) geomagnetic timescale, are presented in Fig.16 (lower panels). There we show that strike-slip motion may have occurred in the

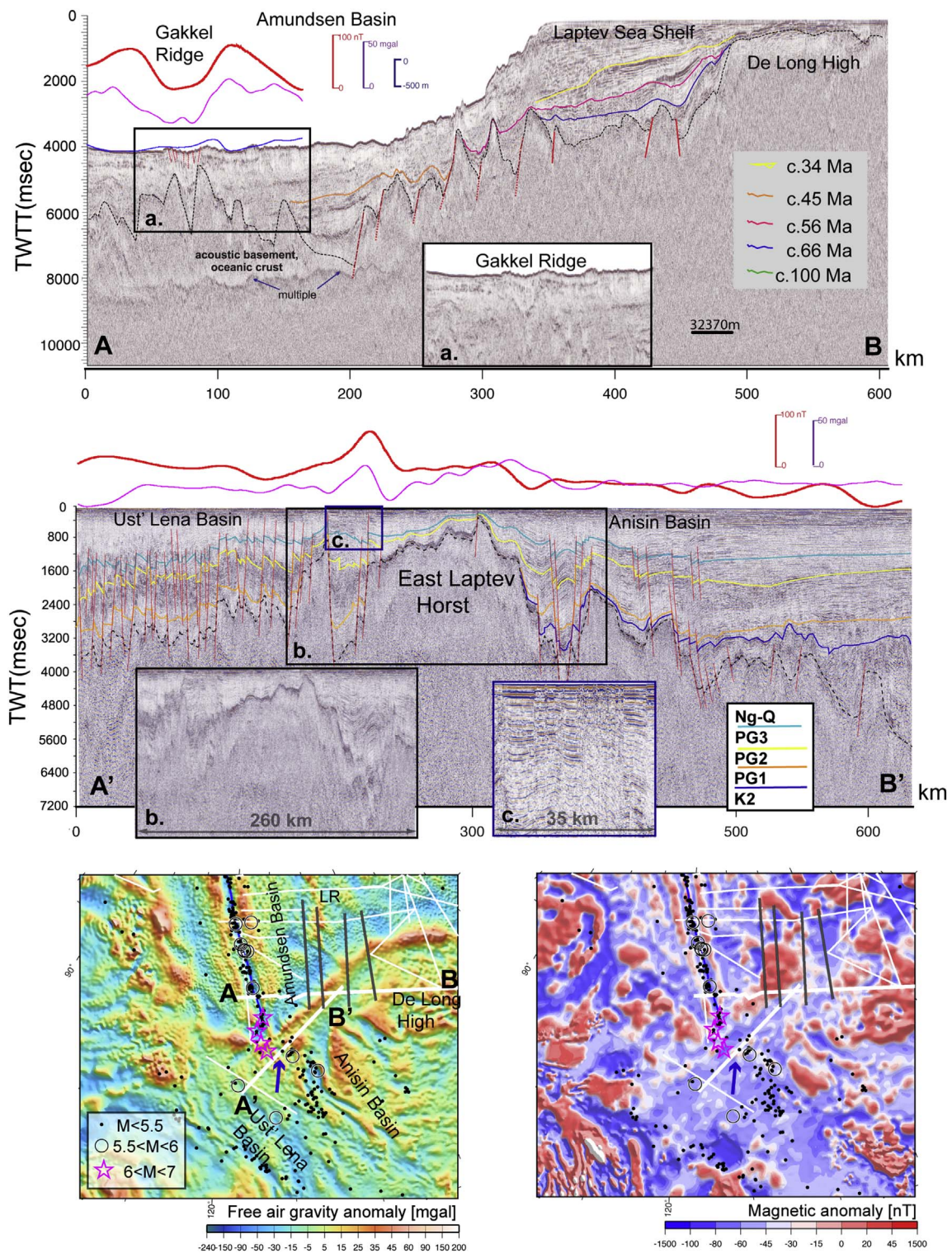


Fig. 15. Seismic lines across the easternmost end of Gakkel Ridge (AB profile: ARC2012-16), and the northernmost part of the Laptev Sea (A'B' profile: ION-11-4600) (location in inset figure and Fig. 1, un-interpreted data in Fig. S6). Lower panels show gravity anomaly (left), and magnetic gridded data (right) as in Fig. 2. Open circles, stars and dots are seismic events from ISC + EMSC earthquake catalogues from 1960 to 2016. Blue arrow indicates the small transform fault that links Gakkel Ridge to the active intra-continental plate boundary in the Laptev Sea.

Abbreviations: K is Cretaceous, PG is Paleogene (PG1-Paleocene, PG2-Eocene, PG3-Oligocene), and Ng-Q is Neogene-Quaternary. LR is Lomonosov Ridge. (For interpretation of the references to colour in this figure legend, the reader is referred to the web version of this article.)

southern Eurasia Basin between break-up time and c. 45 Ma. After that time, transtensional motion was predominant, and perhaps rifting continued in the Ust'Lena Rift, as indicated by thinner (and maybe younger) sediment packages (Fig. 15, profile A'B'). We conclude that

during the opening of the Eurasia Basin, the region at its eastern boundary towards the Laptev Sea shelf, may have acted for a very short time as a strike-slip boundary, but since mid-Eocene it mainly experienced transtension. Today, the Gakkel Ridge is linked by a short

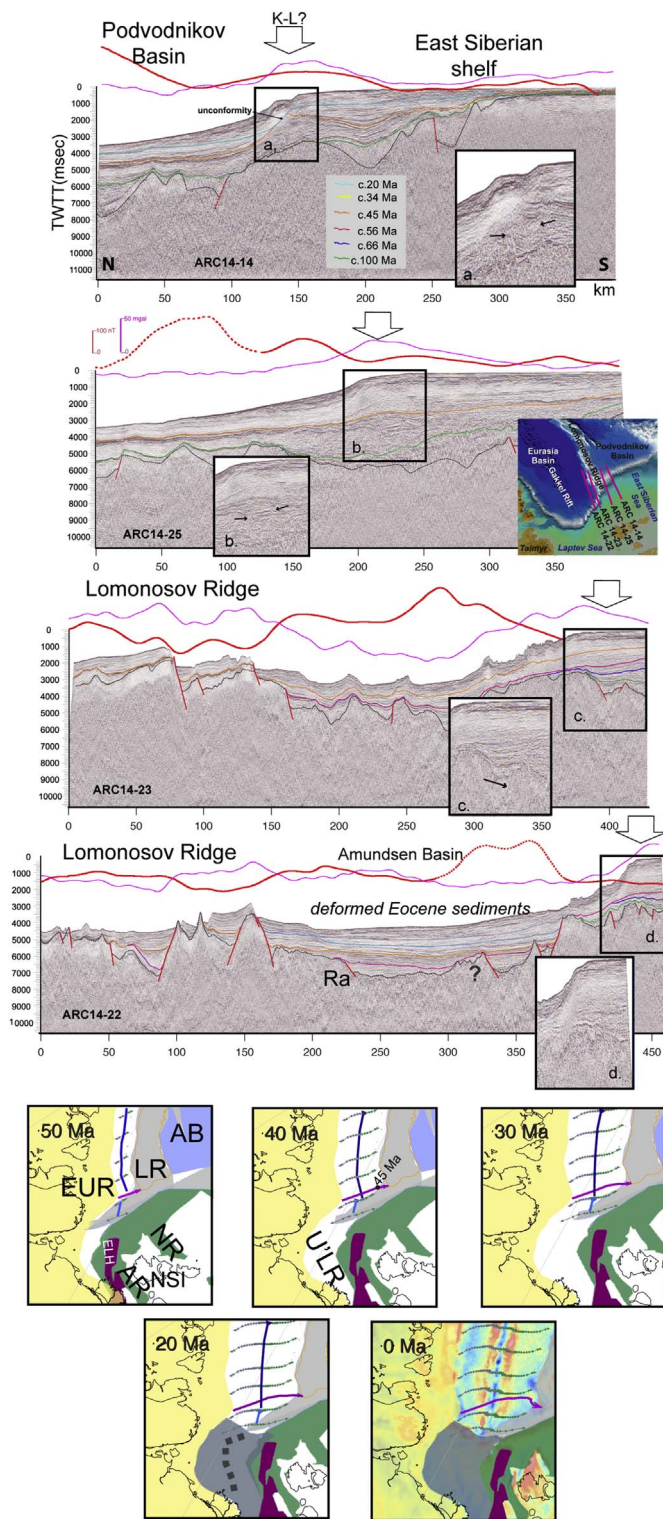


Fig. 16. Seismic lines inspected for Khatanga-Lomonosov Fault (K-L) activity (location in inset figure and Fig. 1, un-interpreted data in Fig. S7). Potential field data and bathymetric profiles as in Fig. 5. Dashed segment in the magnetic profile signals a higher data uncertainty. Lower panels show plate reconstructions of Lomonosov Ridge and adjacent regions (North American plate) relative to a fixed Eurasia (EUR) plate. Abbreviations: AB-Amerasia Basin, AR-Anisin Rift, ELH-East Laptev High, NR-Novosibirsk Rift, NSI-New Siberian Islands, U'LR-Ust'Lena Rift. Blue line is the inferred plate boundary through the Eurasia Basin, light blue line – the inferred continuation of this boundary through northern Laptev Sea, and dashed line is the inferred Oligocene-Miocene intra-continental plate boundary through the Laptev Sea. Magenta line segments show the predicted motion of Lomonosov Ridge (North American plate) relative to Eurasian plate from 55 Ma to Present in 5 myr interval. (For interpretation of the references to colour in this figure legend, the reader is referred to the web version of this article.)

transform with the intra-continental rift that has shifted its location to the east, in the older Anisin Basin (Fig. 15).

6. Conclusions

One of the most extensive modern seismic dataset is documenting, in an unprecedented way, the structure of the youngest High Arctic oceanic basin, the Eurasia Basin, and its margins. In this study we present 25 new seismic profiles in the Nansen and Amundsen basins, their shared mid-ocean ridge, the Gakkel Ridge, and the transition towards the Laptev Sea. The oceanic basement topography imaged by these profiles show two major changes that correspond to variations in seafloor spreading regimes: at C21-20 (45–43 Ma) and at C13 (33 Ma).

This seismic dataset includes a complete, conjugate transect through the entire eastern Eurasia Basin and its margins that allows, for the first time, a quantitative analysis of observed asymmetry in oceanic lithosphere accretion on true conjugate flanks. Continent-ocean boundary location has been interpreted on 9 profiles, and the oldest oceanic lithosphere has been identified on 13 profiles. Asymmetry in oceanic crust accretion occurred both at old and younger seafloor spreading stages in these basins, with a general trend of higher spreading rate in the Nansen Basin, as postulated before (e.g. Jokat and Micksch, 2004). We note that the contrary is true for oceanic lithosphere of C21no-C20no (c. 47–43 Ma), when the report is reversed, at least along the long conjugate profile ARC14-07. The time of change in the seafloor spreading asymmetry coincides with the second peak of the Eureka orogeny and a change in the Arctic Ocean sedimentation pattern dated at c. 45 Ma (e.g. Backman and Moran, 2009), and we suggest that these changes are linked. The seismic profiles in the southern Amundsen Basin show onlapping young sediments against the mid-ocean ridge flanks, indicating an uplift event. The bathymetric scarp that marks this boundary of presumably Oligocene (C13) age is called the “Kazmin Tectonic Scarp”.

A comparison between the detailed structure of the Gakkel mid-ocean ridge and its analogue in the Indian Ocean, SWIR, shows the asymmetry of the ridge flanks and valleys, and similar structures as they approach the pole of rotation and the slowest spreading rate. As in the SWIR case, we observe that the Gakkel Ridge flanks with shallower and rugged structure are more regularly spaced, which may indicate periodic tectonic phases, as suggested by Mendel et al. (2003).

The seismic data presented here reveal new tectonic structures, previously undetected: few seamounts in the Amundsen Basin, a detailed asymmetric structure of the eastern Gakkel Ridge, and a peculiar deep mid ocean ridge valley, the Gakkel Ridge Deep, and its volcanic flanks, formed at the slowest spreading segment of the Gakkel Ridge. From GRD, the Gakkel Ridge continues towards the Laptev Sea as a magmatic segment characterized by high seismicity and occurrence of seamounts, among them the Shaykin and Trubyatchinsky seamounts. In the easternmost part of Eurasia Basin, close to the Laptev Sea shelf, the Gakkel Ridge can be seen as a deep, buried mid-ocean ridge valley, and its current activity is reflected by the recent dense faults that disturb the younger sediments and the seafloor. The Gakkel Ridge is linked with the intra-continental plate boundary, currently east of the Laptev Sea Horst, by a short transform fault segment. Our seismic data and plate tectonic reconstructions suggest that strike-slip motion in the southernmost part of the Eurasian Basin may have occurred from break-up until c. 45 Ma; after that it was mostly transtension between the oceanic and continental domain, probably continuing as rifting in the Ust'Lena basin until very recent. It follows that the Khatanga-Lomonosov transform fault, if present, may have had a shorter than previously postulated life span.

Supplementary Figs. 1–7 show un-interpreted seismic reflection profiles described in the main manuscript and shown in Figs. 5, 6, 8, 9, 11, 15 and 16 respectively. Supplementary data associated with this article can be found in the online version, at <http://dx.doi.org/10.1016/j.tecto.2017.09.006>.

Acknowledgements

The authors are thankful to Ministry of Natural Resources and Ecology of Russia for the possibility to publish this paper. C.G. acknowledges support from The Research Council of Norway through its Centers of Excellence funding scheme, project number 223272. We had many fruitful discussions with Evgeni Burov about the Eurasia Basin and the Gakkell Ridge and regret deeply that he is not with us anymore. Discussions with S. Cloetingh, W. Jokat, E. Miller, and S. Drachev stimulated our work. H. Posamentier, E. Bulgakova, and A. Popova commented on our seismic data interpretation. The authors thank the Editor, and to W. Jokat and an anonymous reviewer for constructive comments and suggestions for language improvement.

References

- Alvey, A., Gaina, C., Kushner, N.J., Torsvik, T.H., 2008. Integrated crustal thickness mapping and plate reconstructions for the high Arctic. *Earth Planet. Sci. Lett.* 274, 310–321.
- Andersen, O.B., Knudsen, P., Kenyon, S., Holmes, S., 2014. Global and Arctic marine gravity field from recent satellite altimetry [DTU13]: extended abstract. In: 76th EAGE Conference Extended Abstracts 2014.
- Backman, J., Moran, K., 2009. Expanding the Cenozoic paleoceanographic record in the Central Arctic Ocean: IODP Expedition 302 synthesis. *Cent. Eur. J. Geosci.* 1 (2), 157–175. <http://dx.doi.org/10.2478/v10085-009-0015-6>.
- Backman, J., Jakobsson, M., Frank, M., Sangiorgi, F., Brinkhuis, H., Stickle, C., O'Regan, M., Lovlie, R., Pällike, H., Spofford, D., Battaceca, J., Moran, K., King, J., Heil, C., 2008. Age model and core-seismic integration for the Cenozoic Arctic Coring Expedition sediments from the Lomonosov Ridge. *Paleoceanography* 23 (1). <http://dx.doi.org/10.1029/2007PA001476>.
- Beal, M.A., Edvalson, F., Hunkins, K., Molloy, A., Ostenso, N., 1966. The floor of the Arctic Ocean: geographic names. *Arctic* 19 (3), 214–219.
- Brozena, J.M., Childers, V.A., Lawver, L.A., Gahagan, L.M., Forsberg, J.I., Faleide, J.I., Eldholm, O., 2003. New aerogeophysical study of the Eurasia Basin and Lomonosov Ridge: implications for basin development. *Geology* 31 (9), 825–828.
- Chernykh, A.A., Krylov, A.A., 2011. Sedimentogenesis in the Amundsen Basin from geophysical data and drilling results on the Lomonosov Ridge. *Dokl. Earth Sci.* 440 (2), 1372–1376.
- Cochran, J.R., 2008. Seamount volcanism along the Gakkell Ridge, Arctic Ocean. *Geophys. J. Int.* 174, 1153–1173. <http://dx.doi.org/10.1111/j.1365-246X.2008.03860.x>.
- Cochran, J.R., Kurras, G.J., Edwards, M.H., Coakley, B.J., 2003. The Gakkell Ridge: bathymetry, gravity anomalies, and crustal accretion at extremely slow spreading rates. *J. Geophys. Res.* 108 (B2), 2116. <http://dx.doi.org/10.1029/2002JB001830>.
- Dick, H.J.B., Lin, J., Schouten, H., 2003. An ultraslow-spreading class of ocean ridge. *Nature* 426, 405–412.
- Donukalova, M.K., 2016. Geological History of Territory of Benett and Kotel'ny Islands in the Early Paleozoic. PhD thesis (candidate dissertation). Geological Institute of Academy of Sciences, Moscow 177 pp. (in Russian).
- Doré, A.G., Lundin, E.R., Gibbons, A., Sømme, T.O., Torudbakken, B.O., 2016. Transform margins of the Arctic: a synthesis and re-evaluation. In: Nemčok, M., Rybár, S., Sinha, S.T., Hermeston, S.A., Ledvényiové, L. (Eds.), *Transform Margins: Development, Controls and Petroleum Systems*. Geological Society, London, Special Publications 431 <http://dx.doi.org/10.1144/SP431.8>.
- Dossing, A., Hansen, T.M., Olesen, A.V., Hopper, J.R., Funck, T., 2014. Gravity inversion predicts the nature of the Amundsen Basin and its continental borderlands near Greenland. *Earth Planet. Sci. Lett.* 408, 132–145. <http://dx.doi.org/10.1016/j.epsl.2014.10.011>.
- Drachev, S.S., 2016. Fold belts and sedimentary basins of the Eurasian Arctic. *Ark. Dent.* 2, 21. <http://dx.doi.org/10.1007/s41063-015-0014-8>.
- Drachev, S.S., Savostin, L.A., Groshev, V.G., Bruni, I.E., 1998. Structure and geology of the continental shelf of the Laptev Sea, Eastern Russian Arctic. *Tectonophysics* 298, 357–393.
- Drachev, S., Malyshev, N., Nikishin, A., 2010. Tectonic history and petroleum geology of the Russian Arctic Shelves: an overview. In: Vining, B.A., Pickering, S.C. (Eds.), *Petroleum Geology: From Mature Basins to New Frontiers – Proceedings of the 7th Petroleum Geology Conference*. Geological Society, London, pp. 591–619. <http://dx.doi.org/10.1144/0070591>.
- Engen, O., Eldholm, O., Bungum, H., 2002. The Arctic plate boundary. *JGR*. <http://dx.doi.org/10.1029/2002JB001809>.
- Engen, Ø., Gjengedal, J.A., Faleide, J.I., Kristoffersen, Y., Eldholm, O., 2009. Seismic stratigraphy and sediment thickness of the Nansen Basin, Arctic Ocean. *Geophys. J. Int.* 176, 805–821. <http://dx.doi.org/10.1111/j.1365-246X.2008.04028.x>.
- Ershova, V.B., Lorenz, H., Prokopyev, A.V., Sobolev, N.N., Khudoley, A.K., Petrov, E.O., Estrada, S., Sergeev, S., Larionov, A., Thomsen, T.B., 2016. The De Long Islands: a missing link in unraveling the Paleozoic paleogeography of the Arctic. *Gondwana Res.* 35, 305–322. <http://dx.doi.org/10.1016/j.jgr.2015.05.016>.
- Franke, D., 2013. Rifting, lithosphere breakup and volcanism: comparison of magma-poor and volcanic rifted margins. *Mar. Pet. Geol.* 43, 63–87. <http://dx.doi.org/10.1016/j.marpetgeo.2012.11.003>.
- Franke, D., Krüger, F., Klinge, R., 2000. Tectonics of the Laptev Sea – Moma 'Rift' region: investigation with seismologic broadband data. *J. Seismol.* 4, 99–116.
- Franke, D., Hinz, K., Oncken, O., 2001. The Laptev Sea Rift. *Mar. Pet. Geol.* 18 (10), 1083–1127.
- Fujita, K., Cambray, F.W., Velbel, M.A., 1990. Tectonics of the Laptev Sea and Moma rift systems, northeastern USSR. *Mar. Geol.* 93 (1–4), 95–118.
- Gaina, C., Roest, W.R., Müller, R.D., 2002. Late Cretaceous-Cenozoic deformation of northeast Asia. *Earth Planet. Sci. Lett.* 197, 273–286.
- Gaina, C., Werner, S.C., Saltus, R., Maus, S., 2011. Circum-Arctic mapping project: new magnetic and gravity anomaly maps of the Arctic. In: Spencer, A.M., Embry, A.F., Gautier, D.L., Stoupakova, A.V., Sørensen, K. (Eds.), *Arctic Petroleum Geology*. Geological Society, London, Memoirs 35. pp. 39–48. <http://dx.doi.org/10.1144/M35.3>.
- Gaina, C., Medvedev, S., Torsvik, T.H., Koulakov, I., Werner, S.C., 2014. 4D Arctic: a glimpse into the structure and evolution of the Arctic in the light of new geophysical maps, plate tectonics and tomographic models. *Surv. Geophys.* <http://dx.doi.org/10.1007/s10712-013-9254-y>.
- Gaina, G., Nikishin, A.M., Petrov, E.I., 2015. Ultraslow spreading, ridge relocation and neotectonic events in the East Arctic region – a link to the Eureka orogeny? *Arktos*. <http://dx.doi.org/10.1007/s41063-015-0006-8>.
- Glebovsky, V.Yu., Kaminsky, V.D., Minakov, A.N., Merkur'ev, S.A., Childers, V.A., Brozena, J.M., 2006. Formation of the Eurasia Basin in the Arctic Ocean as inferred from geohistorical analysis of the anomalous magnetic field. *Geotectonics* 40 (4), 263–281.
- Grachev, A.F., 1983. Geodynamics of the transitional zone from the Moma Rift to the Gakkell Ridge. In: Watkins, J.S., Drake, C.L. (Eds.), *Studies in Continental Margin Geology*. Am. Assoc. Petr. Geol. Mem., vol. 34. pp. 103–114.
- Jakobsson, M., Mayer, L., Coakley, B., Dowdeswell, J.A., Forbes, S., Fridman, B., Hodnesdal, H., Noormets, R., Pedersen, R., Rebeco, M., Schenke, H.W., Zarayskaya, Y., Accettella, D., Armstrong, A., Anderson, R.M., Bienhoff, P., Camerlingh, A., Church, I., Edwards, M., Gander, J.V., Hall, J.K., Hell, B., Hestvik, O., Kristoffersen, Y., Marcussen, C., Mohammad, R., Mosher, D., Nghiem, S.V., Pedrosa, M.T., Travallini, P.G., Weatherall, P., 2012. The International Bathymetric Chart of the Arctic Ocean (IBCAO) Version 3.0. *Geophys. Res. Lett.* 39. <http://dx.doi.org/10.1029/2012gl052219>.
- Jokat, W., Ickrath, M., 2015. Structure of ridges and basins off East Siberia along 81 degrees N, Arctic Ocean. *Mar. Pet. Geol.* 64, 222–232.
- Jokat, W., Micksch, U., 2004. Sedimentary structure of the Nansen and Amundsen basins, Arctic Ocean. *Geophys. Res. Lett.* 31, L26203. <http://dx.doi.org/10.1029/2003GL018352>.
- Jokat, W., Schmidt-Aursch, M., 2007. Geophysical characteristics of the ultraslow spreading Gakkell Ridge, Arctic Ocean. *Geophys. J. Int.* 168, 983–998. <http://dx.doi.org/10.1111/j.1365-246X.2006.03278.x>.
- Jokat, W., Weigelt, E., Kristoffersen, Y., Rasmussen, T., Schone, T., 1995. New insights into the evolution of the Lomonosov Ridge and the Eurasian Basin. *Geophys. J. Int.* 122 (2), 378–392.
- Jokat, W., Ritzmann, O., Schmidt-Aursch, M.C., Drachev, S., Gauger, S., Snow, J., 2003. Geophysical evidence for reduced melt production on the Arctic ultraslow Gakkell mid-ocean ridge. *Nature* 423, 962–965.
- Jokat, W., Kollofrath, J., Geissler, W.H., Jensen, L., 2012. Crustal thickness and earthquake distribution south of the Logachev Seamount, Knipovich Ridge. *Geophys. Res. Lett.* 39, L08302. <http://dx.doi.org/10.1029/2012GL051199>.
- Jokat, W., Ickrath, M., O'Connor, J., 2013. Seismic transect across the Lomonosov and Mendeleev Ridges: Constraints on the geological evolution of the Amerasia Basin, Arctic Ocean. *Geophys. Res. Lett.* 40 (19), 5047–5051.
- Kandilarov, A., Landa, H., Mjelde, R., Pedersen, R.B., Okino, K., Murai, Y., 2010. Crustal structure of the ultra-slow spreading Knipovich Ridge, North Atlantic, along a presumed ridge segment center. *Mar. Geophys. Res.* 31, 173–196. <http://dx.doi.org/10.1007/s11001-010-9095-8>.
- Karasik, A.M., Savostin, L.A., Zonenshain, L.P., 1983. Motion parameters of plates movements in the Eurasian Basin of Arctic Ocean. *Dokl. Akad. Nauk SSSR* 273 (5), 1191–1196 (in Russian).
- Khoroshilova, M.A., Franke, D., Kirillova, T., Mouly, B., Nikishin, A.M., 2014. Dating and correlation of reference seismic horizons in the Laptev Sea Basin. *Mosc. Univ. Geol. Bull.* 69 (5), 271–280. <http://dx.doi.org/10.3103/S0145875214050032>.
- Korger, E.I.M., Schlindwein, V., 2014. Seismicity and structure of the 85° E volcanic complex at the ultraslow spreading Gakkell Ridge from local earthquake tomography. *Geophys. J. Int.* 196, 539–551.
- Kos'ko, M.K., Sobolev, N.N., Korago, E.A., Proskurnin, V.F., Stolbov, N.M., 2013. Geology of Novosibirskian Islands – a basis for interpretation of geophysical data on the Eastern Arctic shelf of Russia. *Neftegasovaa geologiya. Teoriia I practica (RUS)* 8 (2). http://www.ngtp.ru/rub/5/17_2013.pdf.
- Kovacs, L., Glebovsky, V., Sorokin, M., Mashenkov, S., Brozena, J., 1999. New evidence for seafloor spreading in the Makarov Basin. *EOS Trans. Am. Geophys. Union*.
- Kuzmichev, A.B., 2009. Where does the South Anyui suture go in the New Siberian islands and Laptev Sea? Implications for the Amerasia basin origin. *Tectonophysics* 463, 86–108.
- Kvarven, T., Hjelstuen, B.O., Mjelde, R., 2014. Tectonic and sedimentary processes along the ultraslow Knipovich spreading ridge. *Mar. Geophys. Res.* 35, 89–103. <http://dx.doi.org/10.1007/s11001-014-9212-1>.
- Mazur, S., Campbell, S., Green, C., Boutatmeni, R., 2015. Extension across the Laptev Sea continental rifts constrained by gravity modeling. *Tectonics* 34, 435–448. <http://dx.doi.org/10.1002/2014TC003590>.
- Mendel, V., Sauter, D., Rommevaux-Jestin, C., Patriat, P., Lefebvre, F., Parson, L.M., 2003. Magmato-tectonic cyclicity at the ultra-slow spreading Southwest Indian Ridge: evidence from variations of axial volcanic ridge morphology and abyssal hills pattern. *Geochem. Geophys. Geosyst.* 4, 5. <http://dx.doi.org/10.1029/2002GC000417>.

- Merkouriev, S., DeMets, C., 2014. High-resolution quaternary and neogene reconstructions of Eurasia-North America plate motion. *Geophys. J. Int.* 198 (1), 366–384.
- Michael, P.J., Langmuir, C.H., Dick, H.J.B., Snow, J.E., Goldstein, S.L., Graham, D.W., Lehnert, K., Kurras, G., Jokat, W., Mühe, R., Edmonds, H.N., 2003. Magmatic and amagmatic seafloor generation at the ultraslow-spreading Gakkel ridge, Arctic Ocean. *Nature* 423, 956–961.
- Minakov, A., Faleide, J.I., Glebovsky, V.Yu., Mjelde, R., 2012. Structure and evolution of the northern Barents–Kara Sea continental margin from integrated analysis of potential fields, bathymetry and sparse seismic data. *Geophys. J. Int.* <http://dx.doi.org/10.1111/j.1365-246X.2011.05258.x>.
- Moran, K., Backman, J., Brinkhuis, H., Clemens, S.C., Cronin, T., Dickens, G.R., Eynaud, F., Gattaceca, J., Jakobsson, M., Jordan, R.W., Kaminsk, M., King, J., Koc, N., Krylov, A., Martinez, N., Matthiessen, J., McInroy, D., Moore, T.C., Onodera, J., O'Regan, M., Pálik, H., Rea, B., Rio, D., Sakamoto, T., Smith, D.C., Stein, R., St. John, K., Suto, I., Suzuki, N., Takahashi, K., Watanabe, M., Yamamoto, O.M., Farrell, J., Frank, M., Kubik, P., Jokat, W., Kristoffersen, Y., 2006. The Cenozoic palaeoenvironment of the Arctic Ocean. *Nature* 441 (7093), 601–605. <http://dx.doi.org/10.1038/nature04800>.
- More, T.E., Pitman, J.K., 2011. Geology and petroleum potential of the Eurasia Basin. In: Spencer, A.M., Embry, A.F., Gautier, D.L., Stoupakova, A.V., Sørensen, K. (Eds.), *Arctic Petroleum Geology*. Geological Society, London, Memoirs 35. pp. 731–750. <http://dx.doi.org/10.1144/M35.48>.
- Morozov, A.N., Vaganova, N.V., Ivanova, E.V., Konechnaya, Y.V., Fedorenko, I.F., Mikhaylova, Y.A., 2016. New data about small-magnitude earthquakes of the ultraslow-spreading Gakkel Ridge, Arctic Ocean. *J. Geodyn.* 93, 31–41. <http://dx.doi.org/10.1016/j.jog.2015.11.002>.
- Müller, R.D., Sdrolias, M., Gaina, C., Roest, W.R., 2008. Age, spreading rates, and spreading asymmetry of the world's ocean crust. *Geochem. Geophys. Geosyst.* 9 (4).
- Nikishin, A., Amelin, N., Petrov, E., Miles, L., Semb, P.H., Lie, O., Dahl, N., 2013. New 2D seismic data improve evaluation of Barents and Kara Sea basins. *World Oil* 234 (11), 77–80.
- Nikishin, A.M., Malyshev, N.A., Petrov, E.I., 2014. Geological Structure and History of the Arctic Ocean. EAGE Publications bv, PO Box 59, 3990, DB HOUTEN, The Netherlands (88 pp.).
- Nikishin, A.M., Petrov, E.I., Malyshev, N.A., Ershova, V.P., 2017. Rift systems of the Russian Eastern Arctic shelf and Arctic deep water basins: link of geological history and geodynamics. *Geodyn. Tectonophysics* 8 (1), 11–43. <http://dx.doi.org/10.5800/GT-2017-8-1-0231>.
- Ogg, J.G., 2012. The geomagnetic polarity timescale. In: Gradstein, F.M., Ogg, J.G., Schmitz, M., Ogg, G. (Eds.), *The Geologic Time Scale 2012*. Elsevier, Amsterdam, pp. 85–115.
- Okino, K., Curewitz, D., Asada, M., Tamaki, K., Vogt, P., Crane, K., 2002. Preliminary analysis of the Knipovich Ridge segmentation: influence of focused magmatism and ridge obliquity on an ultraslow spreading system. *Earth Planet. Sci. Lett.* 202, 275–288.
- Pease, V., Drachev, S., Stephenson, R., Zhang, X., 2014. Arctic lithosphere – a review. *Tectonophysics* 628, 1–25. <http://dx.doi.org/10.1016/j.tecto.2014.05.033>.
- Petrov, O., Morozov, A., Shokalsky, S., Kashubin, S., Artemieva, I.M., Sobolev, N., Petrov, E., Ernst, R.E., Sergeev, S., Smelror, M., 2016. Crustal structure and tectonic model of the Arctic region. *Earth Sci. Rev.* 154, 29–71. <http://dx.doi.org/10.1016/j.earscirev.2015.11.013>.
- Piskarev, A., Elkina, D., 2017. Giant caldera in the Arctic Ocean: evidence of the catastrophic eruptive event. *Sci. Rep.* 7.
- Poselov, V.A., Avetisov, P., Butsenko, V.V., Zholondz, S.M., Pavlov, S.P., 2012. The Lomonosov Ridge as a natural extension of the Eurasian continental margin into the Arctic Basin. *Russ. Geol. Geophys.* 53, 1276–1290.
- Rekant, P.V., Gusev, E.A., 2012. Seismic geologic structure model for the sedimentary cover of the Laptev Sea part of the Lomonosov Ridge and adjacent parts of the Amundsen Plain and Podvodnikov Basin. *Russ. Geol. Geophys.* 53, 1150–1162. <http://dx.doi.org/10.1016/j.rgg.2012.09.003>.
- Rekant, P.V., Gusev, E.A., 2016. Sediments in the Gakkel Ridge rift zone (Arctic Ocean): structure and history. *Russ. Geol. Geophys.* 57, 1283–1287. <http://dx.doi.org/10.1016/j.rgg.2016.08.013>.
- Rekant, P.V., Petrov, O.V., Kashubin, S.N., Rybalka, A.V., Shokalsky, S.P., Petrov, E.O., Vinokurov, I.Yu., Gusev, E.A., 2015. History of formation of the sedimentary cover of Arctic basin. In: *Multychannel seismic approach. Regional'naya Geologiya I Metallogeniya*. 64. pp. 11–27 (in Russian).
- Savostin, L.A., Karasik, A.M., 1981. Recent plate tectonics of the Arctic basin and of northeastern Asia. *Tectonophysics* 74, 111–145.
- Savostin, L.A., Karasik, A.M., Zonenshain, L.P., 1984. The history of the opening of the Eurasia basin in the Arctic. *Trans. USSR Acad. Sci. Earth Sci. Sect.* 275, 79–83.
- Schindwein, V., Schmid, F., 2016. Mid-ocean-ridge seismicity reveals extreme types of ocean lithosphere. *Nature*. <http://dx.doi.org/10.1038/nature18277>.
- Schindwein, V., Müller, Ch., Jokat, W., 2005. Seismoacoustic evidence for volcanic activity on the ultraslowspreading Gakkel Ridge, Arctic Ocean. *Geophys. Res. Lett.* 32, L18306. <http://dx.doi.org/10.1029/2005GL023767>.
- Schindwein, V., Demuth, A., Korger, E., Läderach, Ch., Schmidt, F., 2015. Seismicity of the Arctic mid-ocean ridge system. *Polar Sci.* 9, 146–157. <http://dx.doi.org/10.1016/j.polar.2014.10.001>.
- Schmidt-Aursch, M., Jokat, W., 2016. 3D gravity modelling off-axis crustal thickness variations along the western Gakkel Ridge (Arctic Ocean). *Tectonophysics* 691, 85–97. <http://dx.doi.org/10.1016/j.tecto.2016.03.021>.
- Sekretov, S.B., 2002. Structure and tectonic evolution of the Southern Eurasia Basin, Arctic Ocean. *Tectonophysics* 351, 193–243.
- Shipilov, E.V., Vernikovskiy, V.A., 2010. The Svalbard-Kara plates junction: structure and geodynamic history. *Russ. Geol. Geophys.* 51 (1), 58–71.
- Snow, J.E., Edmonds, H.N., 2007. Ultraslow-spreading ridges: rapid paradigm changes. *Oceanography* 20 (1), 90–101. <http://dx.doi.org/10.5670/oceanog.2007.83>.
- Sohn, R.A., Willis, C., Humphris, S., Shank, T.M., Singh, H., Edmonds, H.N., Kunz, C., Hedman, U., Helmke, E., Jakuba, M., Liljebldh, B., Linder, J., Murphy, C., Nakamura, K.I., Sato, T., Schindwein, V., Stranne, C., Tausenfrennd, M., Upchurch, L., Winsor, P., Jakobsson, M., Soule, A., 2008. Explosive volcanism on the ultraslow-spreading Gakkel ridge, Arctic Ocean. *Nature* 453, 1236–1238. <http://dx.doi.org/10.1038/nature07075>.
- Sokolov, S.D., Bondarenko, G.Ye., Morozov, O.L., Shekhovtsov, V.A., Glotov, S.P., Ganelin, A.V., Kravchenko-Berezhnoy, I.R., 2002. South-Anyui suture, northeast Arctic Russia: facts and problems. In: Miller, E.L., Grantz, A., Klempere, S. (Eds.), *Tectonic Evolution of the Bering Shelf–Chukchi Sea–Arctic Margin and Adjacent Landmasses. Special Paper*, vol. 360. Geological Society of America, Boulder, Colorado, pp. 209–224.
- Urlaub, M., Schmidt-Aursch, M., Jokat, W., Kaul, N., 2009. Gravity crustal models and heat flow measurements for the Eurasia Basin, Arctic Ocean. *Mar. Geophys. Res.* 30, 277–292. <http://dx.doi.org/10.1007/s11001-010-9093-x>.
- Vogt, P.R., Taylor, P.T., Kovacs, L.C., Johnson, G.L., 1979. Detailed Aeromagnetic Investigation of the Arctic Basin. *J. Geophys. Res.* 84 (Nb3), 1071–1089.
- Weigelt, E., Franke, D., Jokat, W., 2014. Seismostratigraphy of the Siberian Arctic Ocean and adjacent Laptev Sea Shelf. *J. Geophys. Res.* 119 (7), 5275–5289. <http://dx.doi.org/10.1002/2013JB010727>.
- Zavarzina, G.A., Shkarubo, S.I., 2012. Tectonics of the western part of the Laptev sea shelf. *Neftegasovaa geologia. Teoria I praktika* 7 (3) (18 pp.). http://www.ngtp.ru?rub/4/39_2012.pdf.